



# Politecnico di Torino

DIPARTIMENTO DI INGEGNERIA MECCANICA E AEROSPAZIALE  
Corso di Laurea Magistrale in Ingegneria Biomedica

TESI DI LAUREA MAGISTRALE

## Development of a platform for drug screening studies through cell-substrate impedance sensing

Candidata:  
**Emilj PERRONE**

Relatore:  
**Prof. Danilo DEMARCHI**

Correlatori:  
**Dott. Alessandro SANGINARIO**  
**Dott.ssa Sharmila FAGOONEE**

Settembre 2018



**POLITECNICO  
DI TORINO**

Università di Torino



Molecular Biotechnology Center



# Ringraziamenti

Molte persone hanno contribuito alla realizzazione e alla conclusione del mio percorso universitario.

Innanzitutto, desidero ringraziare il prof. Danilo Demarchi, per avermi permesso, con la disponibilità e la cordialità che lo contraddistinguono, di intraprendere il mio progetto di Tesi Magistrale.

Ringrazio la prof.ssa Fiorella Altruda, del Molecular Biotechnology Center (MBC), per avermi dato fiducia accogliendomi nel suo laboratorio e permettendomi di utilizzare tutto il materiale necessario allo svolgimento dei miei esperimenti.

Desidero inoltre ringraziare il dott. Alessandro Sanginario, sempre pronto a fornirmi chiarimenti nei momenti di difficoltà.

Un grande ‘grazie’ lo rivolgo alla dott.ssa Sharmila Fagoonee, mia tutor all’MBC, con la quale ho passato abbastanza tempo da poterla definire ormai un’amica e dalla quale ho imparato tantissimo.

Ringrazio inoltre il gentilissimo dott. Paolo Squillari, per il grande aiuto fornitomi in alcune fasi dello sviluppo software del mio progetto di tesi.

Un ‘grazie’ speciale lo merita senza ombra di dubbio l’ing. Gianfranco Albis, che definisco affettuosamente il mio ‘psicologo’ e a cui ho spesso raccontato i miei problemi universitari, ricevendo sincero ascolto e consigli paterni. Mi ha insegnato tanto e con gentilezza e disponibilità mi ha sempre sostenuta, credendo in me.

Ringrazio il Politecnico, perché proprio qui ho stretto amicizie forti, ho conosciuto persone autentiche. Prime tra tutte Valentina e Adele, semplicemente uno dei più bei regali che quest’avventura potesse farmi. Grazie a Carmen e Lucia, due amiche sincere oltre che compagne di viaggio. Grazie a Gianluca, amico vero e fidato, per avermi strappato un sorriso nei momenti bui di questo percorso.

Grazie agli amici di sempre, che c’erano, ci sono e resteranno.

Grazie a mamma e papà, il cui contributo alla realizzazione di tutto questo è inquantificabile. Ringrazio mio padre per avermi continuamente spronata a non arrendermi e per ogni “ma tanto lo sapevo già” quando gli comunicavo di aver superato un esame; ringrazio mia madre per aver sempre asciugato le mie lacrime e per le lunghissime chiacchierate al telefono per sentirsi più vicina a me. Grazie ai miei fratelli, la mia vita. Grazie alla mia grande famiglia, per essere quella che è, semplicemente unica.

Ringrazio Gabriele, per avermi sopportata e supportata sempre, per aver condiviso con me tutte le emozioni che questo percorso mi ha riservato, nonostante 1200 chilometri ci separassero.



# Abstract

My master thesis project stems from the beginning of a collaboration between Politecnico di Torino and the Molecular Biotechnology Center (MBC) of the University of Turin.

The aim of my project is the development of a platform for impedance measurements on cell cultures, finalised to *drug screening* studies. Changes of an electrical parameter as impedance reflect changes in the cells status: in particular, an increase in impedance is index of viability and proliferation, while an impedance decrease represents cell death.

To this aim, a commercial device, the BioChip 4096E (*3Brain* GmbH, Switzerland) was used and seeded with cells, since its design integrates the presence of a culture chamber and a certain number of electrodes, giving the possibility to conduct impedance measurements.

The part of the work related to the experimental measurements set up was developed at Politecnico di Torino: an impedance analyzer (Agilent 4294A) was used to execute the measurements and a program in LabVIEW® 2017 was created to open the communication with the instrument and allow the user to set all the parameters for conducting the measurements directly from a friendly Graphical User Interface (GUI). Moreover, since 16 electrodes are available but only a couple is necessary for one measurement, the user has also the possibility to choose through the GUI the couple of electrodes for the current measurement session.

The part related to the cell seeding on the BioChip 4096E was conducted at the MBC: HT-29 cell line from colorectal cancer was used and the optimization of the protocols for ensuring adhesion and viability of cells on the electrodes area was performed.

Once adhesion and proliferation of cells in the BioChip's culture chamber were established, an apoptosis inducer (Etoposide) was added to the cell culture to analyse whether drug screening tests could be performed with the colorectal cancer cell line, used for the first time on this BioChip.

By monitoring impedance evolution over time, cell adhesion, proliferation and death (as a result of the apoptosis inducer addition) were assessed. Data derived from the measurements were saved and analyzed in Matlab® R2018a.

The results obtained showed a dose-dependent cell death degree and demonstrate that impedance monitoring may be a real-time, label-free and non-invasive method for drug screening tests.



# Contents

<b>1</b>	<b>Introduction</b>	<b>19</b>
1.1	Apoptosis: preliminar notions . . . . .	19
1.2	Apoptosis dysregulation in cancer . . . . .	22
1.3	Targeting apoptosis in cancer treatment . . . . .	23
1.4	Aim of the thesis work . . . . .	24
1.5	Electric Cell-substrate Impedance Sensing (ECIS) . . . . .	25
1.5.1	Electric model of a cell . . . . .	25
1.5.2	What is impedance? . . . . .	25
1.5.3	How can cell impedance be measured? . . . . .	26
1.5.4	Parameters influencing cell impedance measurements . . . . .	27
<b>2</b>	<b>State of the art</b>	<b>31</b>
2.1	The drug development process . . . . .	31
2.2	Current drug screening tests . . . . .	32
2.3	Platforms for drug screening tests by impedance measurements . . . . .	34
<b>3</b>	<b>Experimental set-up</b>	<b>37</b>
3.1	<i>3Brain</i> BioChip 4096E . . . . .	38
3.1.1	General features . . . . .	38
3.1.2	BioChip 4096E sterilization and cleaning protocols . . . . .	40
3.2	HT-29 cell line . . . . .	41
3.2.1	General features . . . . .	41
3.2.2	Thawing protocol . . . . .	43
3.2.3	Freezing protocol . . . . .	44
3.2.4	Subculturing protocol . . . . .	44
3.3	HT-29 cell culture protocol on BioChip 4096E . . . . .	45
3.4	Apoptosis inducer: Etoposide . . . . .	46
3.5	Agilent 4294A Precision Impedance Analyzer . . . . .	47
3.6	Arduino® Micro and CD4067 multiplexers . . . . .	50
<b>4</b>	<b>Impedance Measurements and data elaboration</b>	<b>59</b>
4.1	Experiments timeline . . . . .	59
4.2	LabVIEW® Graphical User Interface . . . . .	60
4.2.1	Settings configuration . . . . .	62
4.2.2	Single measurement . . . . .	63
4.2.3	Impedance monitoring over time . . . . .	66

<b>5</b>	<b>Results and discussion</b>	<b>71</b>
5.1	Evaluation of the cellular adhesion and proliferation . . . . .	71
5.1.1	Validation assay . . . . .	74
5.2	Evaluation of the effect of Etoposide . . . . .	75
5.2.1	Validation assay . . . . .	79
<b>6</b>	<b>Conclusions and future perspectives</b>	<b>83</b>
	<b>Bibliography</b>	<b>85</b>

# List of Figures

1.1	<b>Caspases activation pathways: intrinsic and extrinsic.</b> [4] . . . . .	21
1.2	<b>Phenomena involved in the apoptosis dysregulation in cancer.</b> [4] .	23
1.3	<b>Schematic explanation of cells opposition to a current flow.</b> [10] .	25
1.4	<b>Electric model of a cell layer above an array of electrodes.</b> The grey bodies represent adjacent cells. In addition to the single cell resistance ( $R_{Cell}$ ) and cell capacitance ( $C_{Cell}$ ), the resistances associated respectively to cell-cell junctions ( $R_{Junc}$ ), to the culture medium ( $R_{Med}$ ), to the space between cells and electrodes ( $R_{Sub}$ ) and the parallel circuit formed by the resistance ( $R_{Electr}$ ) and the capacitance ( $C_{Electr}$ ) of the electrode-electrolyte interface must be considered. [11] . . . . .	27
1.5	<b>Cells behaviour at low frequencies current (&lt; 2 kHz).</b> Since cell reactance increases, the current passes through the junction between adjacent cells. [14] . . . . .	28
1.6	<b>Cells behaviour at high frequencies current (&gt; 40 kHz).</b> Since cell reactance decreases, the current passes through the cell body. [14] . . . . .	28
1.7	<b>Schematic representation of cell-electrode interaction.</b> As the electrode's covered area increases, impedance increases. [15] . . . . .	29
2.1	<b>Drug development timeline.</b> The funnel represents the number of compounds which succeed from one phase to the next; averagely, one compound over several thousands is placed on the market. [16] . . . . .	32
2.2	<b>Materials and architecture of each microelectrode in a CMOS-based MEA (multi electrode array).</b> [21] . . . . .	34
2.3	<b>xCELLigence® system design.</b> Six 96-well plates can be monitored at the same time; the parameters are set through the dedicated User Interface. [10] . . . . .	35
2.4	<b>Expected impedance curve from xCELLigence® system.</b> The system can provide information about several cells activities, i.e. adhesion, proliferation and death in presence of a toxic agent. [10] . . . . .	35
3.1	<b>Scheme reporting the experimental set-up for the automated impedance measurements.</b> . . . . .	38
3.2	<b>Design of BioChip 4096E (3Brain).</b> [26] . . . . .	39
3.3	<b>Schematic representation of recording and stimulation electrodes arrangement on the chamber's flat area.</b> [27] . . . . .	39
3.4	<b>Scanning electron microscopy (SEM) image showing the electrodes morphology.</b> A cell adhered on the electrodes surface can be seen. [28] . . . . .	40

3.5	<b>Growth curve for cultured cells.</b> Initially a slow growth (lag phase) is verified; then an exponential growth phase occurs (log phase) and it terminates when a plateau is reached (stationary phase), indicating that cells are not proliferating anymore. The correct moment for subculturing cells is indicated in figure. [32] . . . . .	42
3.6	<b>Preparation of the culture medium through a Corning® Bottle-Top Vacuum Filter System (<i>Sigma</i>).</b> . . . . .	43
3.7	<b>Chip's accomodation for preconditioning phase.</b> The BioChip 4096E is placed into the big Petri dish, which is closed, together with the smaller cell culture dishes, filled with DDW to preserve humidity. Then the chamber is filled with culture medium and the system is incubated for 48 hours. . . .	46
3.8	<b>Electric model for impedance measurements by 4294A impedance analyzer.</b> The device under test is connected to the high and low terminals of the instrument and the impedance value is obtained from the ratio between the generated voltage and the measured current. [38] . . . . .	47
3.9	<b>Equivalent circuit of the DUT-fixtures interface.</b> The test fixture leads are characterized by lead inductances ( $L_L$ ), lead resistances ( $R_L$ ), eventual stray capacitances ( $C_0$ ) and contact resistances ( $R_C$ ). [38] . . . . .	48
3.10	a) <b>Front panel view of 4294A precision impedance analyzer (Agilent) [39];</b> b) <b>Design of the Agilent 16089B Kelvin Clip Leads [40].</b> . . . .	49
3.11	<b>Image of the 16-wires flat cable soldered to the 3Brain BioChip 4096E pads corresponding to the stimulation electrodes.</b> The connections are at the end covered by a layer of silicone to isolate them from the external environment and strengthen them against humidity, since the system must stay in incubation at 37°C. . . . .	49
3.12	a) <b>Terminal assignment for Arduino® Micro. [43];</b> b) <b>Terminal assignment for CD4067B CMOS Analog multiplexer. [42]</b> . . . . .	51
3.13	<b>Electrical scheme of the circuit created.</b> . . . . .	51
3.14	<b>Electronic circuit created for choosing the electrodes for the impedance measurements.</b> . . . . .	52
3.15	<b>LED matrix created in LabVIEW® to let the user choose the electrodes for conducting the impedance measurements directly from LabVIEW® grapgical user interface.</b> . . . . .	54
3.16	<b>Comparison between the indexing of the real electrodes in the BioChip 4096E and of the LEDs in LabVIEW®.</b> In the first case the indexing starts from the lower left corner, while in the second case it starts from the upper left corner. . . . .	54
3.17	<b>Conversion table used in the Arduino program.</b> . . . . .	55
3.18	<b>General flowchart of the Arduino® program working principle.</b> BLOCK 1 and BLOCK 2 are explained in detail in the next flowcharts. . . .	56
3.19	<b>Flowchart of the "switch case" instruction executed for the conversion of the first number read from the string (BLOCK 1).</b> . . . .	57
3.20	<b>Flowchart of the "switch case" executed for the conversion of the second number read from the string (BLOCK 2).</b> . . . . .	58
4.1	<b>Timeline followed for assessing cells adhesion on the BioChip 4096E.</b>	59
4.2	<b>Timeline followed for evaluating the effect of the drug on the cell culture in the BioChip 4096E.</b> . . . . .	60
4.3	<b>General flowchart explaining the operations executed by the LabVIEW® program for the impedance measurements.</b> . . . . .	61

4.4	"Settings" page of the tab control in the LabVIEW® GUI. . . . .	62
4.5	Content of the <i>subVI_configuration</i> for impedance single measurement. . . . .	64
4.6	Content of the <i>subVI_sendTrigger</i> . . . . .	64
4.7	Extract of the structure of the text document created after each measurement. . . . .	65
4.8	"Single measurement" page of the tab control in the LabVIEW® GUI. . . . .	65
4.9	Theoretical trend of the overlapped impedance curves when the chip's chamber is filled with medium or seeded with cells. After plotting this graph, the frequency at which the maximum difference between the curves is found, is chosen as the stimulation frequency for the subsequent monitoring phase. [25] . . . . .	66
4.10	Content of the <i>subVI_configuration</i> for impedance monitoring over time. . . . .	68
4.11	"Monitoring over time" page of the tab control in the LabVIEW® GUI. . . . .	68
4.12	Theoretical trend of impedance modulus in the case of monitoring over time. The value $Z_0$ represents measured impedance on the chip without cells; the value $Z_1$ is the measured impedance in presence of cells adhered on the electrodes surface. As can be seen, $Z_1 > Z_0$ . [14] . . . . .	69
5.1	Matlab® plots of the overlapped curves referred to impedance measured with and without cells for assessing cells adhesion. The frequency sweep was executed from 100 Hz to 200 kHz and different voltage values were tested (5, 10, 50, 100 mV). . . . .	72
5.2	Matlab® plot of the impedance monitoring curve for assessing cells proliferation. The measures were executed every 15 minutes for 120 hours. . . . .	73
5.3	Eclipse 80i (Nikon) fluorescence microscopy images (20X) for evaluating cellular adhesion on the BioChip's surface. The results of two tests are reported: a) 90000 cells, collagen 5 $\mu g/mL$ ; b) 50000 cells, laminin 10 $\mu g/mL$ , collagen 10 $\mu g/mL$ . . . . .	75
5.4	Zeiss Microscopy images (20 X) of the eight culture wells treated with Etoposide. a) ETO 0 $\mu M$ ; b) 5 $\mu M$ ; c) 10 $\mu M$ ; d) 20 $\mu M$ ; e) 40 $\mu M$ ; f) 60 $\mu M$ ; g) 80 $\mu M$ ; h) 100 $\mu M$ . . . . .	77
5.5	Impedance curves obtained from the monitoring of the BioChip's cell culture treated with Etoposide. Different concentrations were tested: 0 $\mu M$ , 10 $\mu M$ , 20 $\mu M$ , 40 $\mu M$ , added to the case of culture medium without cells. . . . .	78
5.6	a) Design of the Muse® Cell Analyzer [50]; b) Example of the results provided by the instrument's analysis [49]. . . . .	80
5.7	Results of the Muse™ Cell Analyzer analysis. a) ETO 0 $\mu M$ ; b) 5 $\mu M$ ; c) 10 $\mu M$ ; d) 20 $\mu M$ ; e) 40 $\mu M$ ; f) 60 $\mu M$ ; g) 80 $\mu M$ ; h) 100 $\mu M$ . . . . .	81
5.8	Bar graph showing the apoptotic cells percentages for each sample analysed. . . . .	82



# List of Tables

2.1	Principal drug cytotoxicity assays. [18]	33
2.2	Advantages and disadvantages of ECIS compared to the MTT assay. [12][25]	36
3.1	Resuming table of all the dimensions of BioChip 4096E. [27]	39
3.2	HT-29 cell line features. [30]	41
3.3	Arduino® Micro technical specifications. [41]	50
3.4	CD4067B multiplexer technical specifications. [42]	50
3.5	CD4067B multiplexer truth table. [42]	53
4.1	Resuming table of all the commands set in 4294A for configuring the device to ECIS measurements (single measurements).	63
4.2	Resuming table of all the commands set in 4294A for configuring the device to ECIS measurements (impedance monitoring over time).	67
5.1	Table reporting all the combinations tested for improving cellular adhesion on the BioChip's surface.	71
5.2	Populations of cells which can be distinguished by the Guava Nexin® Assay. [49]	79



# List of Abbreviations

**MBC** Molecular Biotechnology Center

**GUI** Graphical User Interface

**PS** Phosphatidylserine

**DISC** Death inducing signalling complex

**TNF** Tumor Necrosis Factor

**TNFR** Tumor Necrosis Factor Receptor

**DIABLO** Direct IAP Binding protein with Low pI

**IAP** Inhibitor of apoptosis protein

**MOMP** Mitochondrial Outer Membrane Permeabilization

**TRAIL** TNF-Related Apoptosis-Inducing Ligand

**CMOS** Complementary Metal-Oxide Semiconductor

**MEA** Multi Electrode Array

**ECIS** Electric Cell-substrate Impedance Sensing

**RC** Resistor-Capacitor

**DC** Direct Current

**AC** Alternating Current

**IFC** Impedance Flow Cytometry

**EIS** Electric Impedance Spectroscopy

**FDA** Food and Drug Administration

**IND** Investigational New Drug

**NDA** New Drug Application

**HTS** High Throughput Screening

**RTCA** Real-Time Cell Analysis

**CI** Cell Index

**PCB** Printed Circuit Board  
**SEM** Scanning Electron Microscopy  
**DDW** Double Distilled water  
**PBS** Phosphate Buffered Saline  
**FBS** Fetal Bovine Serum  
**PS** Penicillin-Streptomycin  
**DMSO** Dimethyl Sulfoxide  
**ETO** Etoposide  
**DUT** Device Under Test  
**4TP** Four-Terminal Pair  
**LED** Light Emitting Diode  
**IDE** Integrated Development Environment  
**VI** Virtual Instrument  
**GPIB** General Purpose Interface Bus  
**VISA** Virtual Instrument Software Architecture  
**CFDA SE** Carboxyfluorescein diacetate succinimidyl ester  
**TMR** Tetramethylrhodamine  
**dUTP** Deoxyuridine Triphosphate  
**TdT** Terminal Deoxynucleotidyl Transferase  
**TUNEL** TdT-mediated dUTP nick end labeling

# Chapter 1

## Introduction

### 1.1 Apoptosis: preliminar notions

Currently, three types of cell death are recognized: apoptosis (or type I cell death), cell death associated with autophagy (type II cell death) and necrosis (type III cell death) [1]. Autophagy occurs when cells suffer from the absence of nutrients and growth factors and it is properly a survival mechanism: when cells do not dispose of energy sources, the cytoplasmic components are transported by a structure named the autophagosome into the lysosomes, where they are degraded and recycled. This leads to the formation of new products (lipids, aminoacids, carbohydrates) for the synthesis of new proteins or for obtaining energy supply [2]. In some cases, when cells are excessively stressed, autophagy can result in apoptosis or necrosis [1].

Apoptosis and necrosis are the main cell death mechanisms and they strongly differ in terms of cell morphology and signaling pathways. Necrosis is an uncontrolled and passive process, which occurs in case of osmotic shocks, cells exposure to heat, mechanical stresses, presence of poisons and toxins or high concentrations of hydrogen peroxide ( $H_2O_2$ ). In these conditions, a series of morphological changes can occur, for example the creation of cytoplasmic vacuoles or cytoplasmic blebs, the rupture of mitochondria or lysosomes, the detachment of ribosomes, the rupture of organelle membranes, and generally the rapid rupture of the plasma membrane occurs, resulting in the release of cellular material which induces an inflammatory response by the immune system [1][3].

Apoptosis, also called "programmed cell death", was described for the first time by Kerr *et al* in 1970 and it is instead a controlled, predictable and energy-dependent death process, which is a physiological mechanism for eliminating damaged cells and maintaining the homeostasis between cell proliferation and cell death in tissues. It is estimated that every day in an adult human body 10 billion cells must be produced for balancing cells dead for apoptosis [3].

Apoptotic cells show well-defined morphological changes, such as plasma membrane blebbing, chromatin condensation, nuclear fragmentation and formation of apoptotic bodies. These changes are accompanied by the reduction of the cellular volume and the retraction of the pseudopodes, resulting in a cellular rounding-up. In apoptotic mechanisms, differently from necrosis, the inflammatory response does not occur; the reason is that apoptotic cells are phagocytosed by phagocytic cells before the apoptotic bodies are released. Infact, apoptotic cells are recognized by phagocytes thanks to the expression of phosphatidylserine (PS) in the extracellular domain of the plasma membrane, which in general is expressed only in the cytoplasmic domain. PS is externalized in the earliest stages of apoptosis, allowing an early recognition and avoiding the immune response. In

the *in vitro* condition phagocytic cells are not present, hence the apoptotic bodies are visible and their degradation is similar to necrosis: for this reason this is called secondary necrosis [4].

Apoptosis is strongly correlated to the activation of caspases, enzymes of the cysteine protease family. The first letter of their name is referred to cysteine, “asp” is instead referred to the property of cleaving after an aspartic acid residue, “ase” means that they are enzymes. When caspases are activated, they can cleave many proteins, activate DNAase (whose role is DNA degradation) or damage nucleus or cytoskeleton.

Caspases may be activated through two possible pathways, the intrinsic one and the extrinsic one, both terminating with apoptosis.

The extrinsic pathway, also named extrinsic death receptor pathway, is activated when the cell receives external death signals, i.e. when death ligands bind to the death receptors expressed on the plasma membrane. Since in their intracellular domain these receptors communicate with adaptor proteins, such as caspase 8, a complex ligand-receptor-adaptor protein, called death inducing signalling complex (DISC) is created and a signaling cascade is activated. In this pathway, pro-caspase 8 is activated becoming caspase 8 and can activate other caspases, such as pro-caspase 3 to caspase 3, starting the apoptosis process. The most important death ligand is the so called tumor necrosis factor (TNF) and its membrane receptor is the TNF receptor (TNFR).

The intrinsic pathway, or mitochondrial pathway is instead activated in case of internal stimuli, such as irreversible genetic damages, oxidative stresses, high cytosolic  $Ca^{2+}$  concentrations, hypoxia. These stimuli interfere with mitochondria activities, regulating their permeability and the release of cytochrome-c (a pro-apoptotic molecule) into the cytoplasm. This pathway is controlled by a family of proteins called Bcl-2, which can be divided into two categories: the pro-apoptotic Bcl-2 proteins increase the mitochondria permeability promoting the release of cytochrome-c and consequently apoptosis, while the anti-apoptotic proteins reduce the mitochondria permeability, impeding the cytochrome-c release. Cytochrome-c forms with pro-caspase 9 an apoptosome, a complex which activates pro-caspase 3 to caspase 3. Besides cytochrome-c, other factors are released by mitochondria, which form other complexes that lead to the activation of caspase 3 or 9. Initially these caspases are connected to the inhibitors of apoptosis proteins (IAPs), but when an apoptosis factor is present, it binds to the IAPs promoting the rupture of the bond between the IAPs and the caspases and activating them. Additional apoptosis factors to cytochrome-c are Smac (second mitochondria-derived activator of caspase) and DIABLO (direct IAP Binding protein with Low pI) [4].

The intrinsic and extrinsic pathways for cell apoptosis are presented in figure 1.1.

As can be deduced from the previous explanation, the intrinsic and extrinsic pathways activate respectively caspase 9 and caspase 8, but in the end they both activate caspase 3, so these two different pathways produce the same effect downstream. Caspases 8 and 9 belong to the groups of initiator caspases, responsible of the apoptosis pathways initiation, while caspase 3 belongs to the group of effector caspases, which play their cleavage function while apoptosis occurs [4].

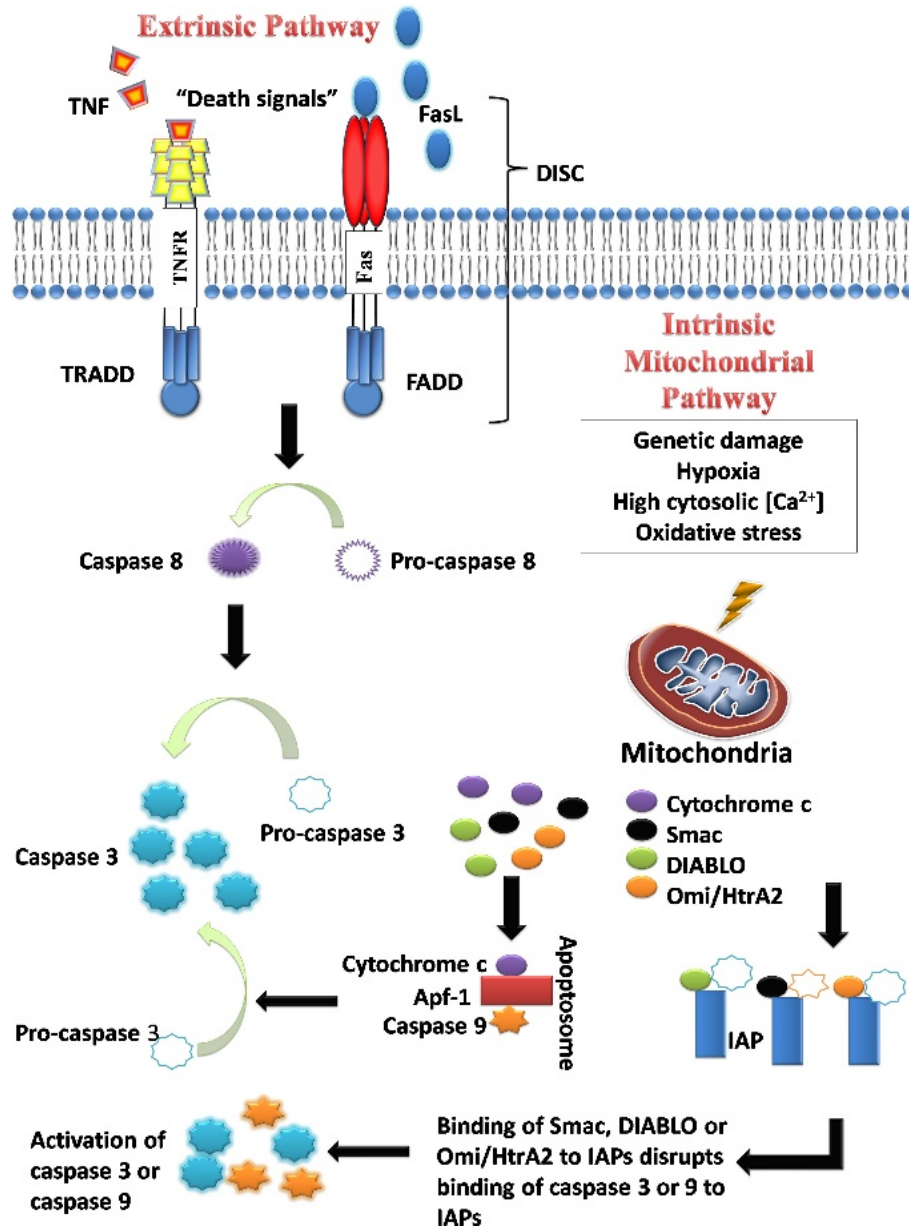


Figure 1.1: Caspases activation pathways: intrinsic and extrinsic. [4]

## 1.2 Apoptosis dysregulation in cancer

Generally, a pathological situation occurs when the balance between proliferating cells and dying cells is compromised, both in case of apoptosis excess and in case of apoptosis insufficiency. In pathological mechanisms the intrinsic pathway for caspase activation is mainly affected, due to an over- or under-expression of the anti- and pro-apoptotic factors. For instance, neurodegenerative and autoimmune diseases, such as Alzheimer's disease and AIDS, are characterized by an apoptosis excess regarding respectively neurons and T cells [3].

Apoptosis also plays a crucial role in tumorigenesis. Cancer is the result of a series of genetic modifications which lead a healthy cell to become a tumor cell. Tumors are characterized by an apoptosis insufficiency; infact, the major phenomenon in tumors is the unbalance between cells proliferation and cells apoptosis. Many factors can lead to the inhibition of apoptosis intrinsic pathways in cancer cells [4][5]:

- In 50 % of human cancers a mutation of the *p53* tumor suppressor gene was found, which is the gene responsible of the regulation of the apoptotic factors expression: it regulates the expression of Bax, a pro-apoptotic protein from the Bcl-2 family, whose activation leads to the mitochondrial outer membrane permeabilization (MOMP), hence to apoptosis. *p53* can also recognize and repair DNA damages and give birth to apoptosis signalling pathways if the damage is irreversible. When this gene is mutated, many functions such as cell cycle regulation, differentiation, DNA amplification and recombination are compromised, too little apoptosis occurs, hence the capability of tumor suppression fails.
- Another possible cause for apoptosis dysregulation in cancer may be associated to an over-expression of the Inhibitor of Apoptosis proteins (IAPs), which keep the pro-caspases bonded for preventing their activation or degrade them.
- Moreover, a dysregulated expression of initiator and effector caspases may also lead to infrequent apoptosis. For instance, in some tumors an under-expression of caspase 9, an apoptosis initiator, and of caspase 3, an apoptosis effector, were encountered.

With regard to the extrinsic pathway for apoptosis initiation, different issues may occur:

- The death receptors of the plasma membrane may lack of the intracellular death domain as consequence of mutations; in this case the DISC complex cannot be created and the signalling cascade for activating caspase 3 cannot be realized.
- In some cases the death receptors are under-expressed on the cell membrane, making it difficult to activate the signalling cascade.

Figure 1.2 schematically reports the causes of apoptosis dysregulation in cancer.

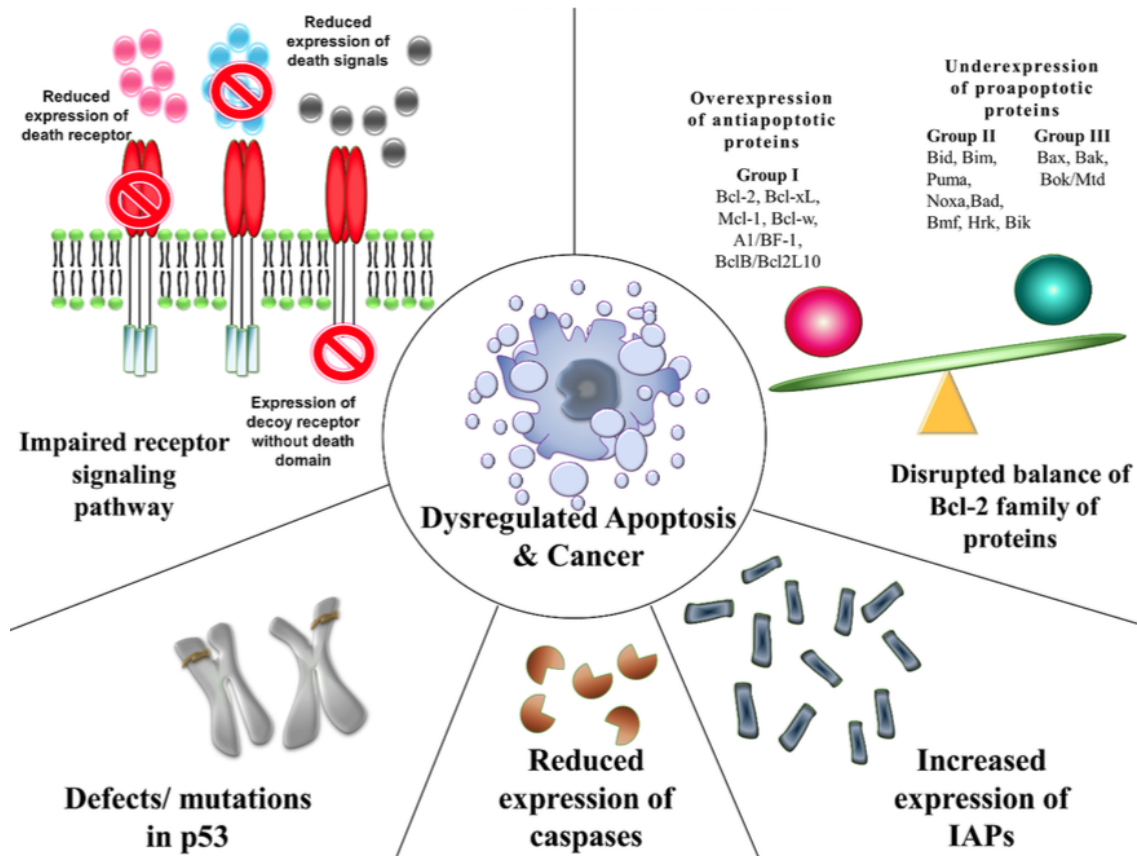


Figure 1.2: Phenomena involved in the apoptosis dysregulation in cancer. [4]

### 1.3 Targeting apoptosis in cancer treatment

Understanding the apoptosis inhibition mechanisms in tumors is strongly important for developing new anticancer agents and treatments that induce apoptosis in tumor cells. Today most of anticancer drugs act on DNA by interfering with its mechanisms, such as replication and cell division. In this case apoptosis is induced by the irreversible DNA damages. There is a great number of chemotherapeutic drugs, which can be grouped in six categories, depending on their action mechanism [6]:

- **Alkylating agents:** they act in different phases of the cell cycle by binding to the DNA, impeding the protein synthesis and implying apoptosis.
- **Antimetabolites:** they mainly act by replacing the standard DNA or RNA building blocks and preventing the synthesis of new nucleotides.
- **Anti-tumor Antibiotics:** they are specific antibiotics targeted to prevent growth and proliferation of cancer cells by interfering with some enzymes during their DNA replication.
- **Topoisomerase inhibitors:** they are particular agents that interfere specifically with the enzymes Topoisomerase I and II, involved in the DNA replication.
- **Mitotic inhibitors:** they are typically substances derived by plants, which damage DNA during the cell division.

- **Corticosteroids:** they are simply hormones, which in several cases can work as chemotherapeutic drugs.

The risk of using drugs targeted to DNA is their low specificity for tumor cells; in fact also healthy cells are involved in the apoptosis process [7]. The current ideas for improving anticancer treatments and for making them specific towards cancer cells may be aimed to the previously explained mutations that induce apoptosis inhibition [4][5][7]:

- **Targeting anti-apoptotic proteins:** numerous studies have demonstrated that by silencing the genes which code the Bcl-2 anti-apoptotic proteins with a specific siRNA sequence (small interfering RNA), apoptosis occurs. Another way for inducing apoptosis is to use drugs called BH3 mimetics, because *in vivo* BH3-only proteins inhibit the action of Bcl-2 anti-apoptotic proteins.
- **Targeting *p53*:** a group of drugs exists for restoring the mutated *p53* genes to their original form. In addition to drug therapy, a gene therapy can be developed by adenoviral transfer of a wild-type *p53* gene into cancer cells presenting mutations in *p53*.
- **Targeting the IAPs:** even in this case, silencing IAPs has proved to be effective, with apoptosis occurrence. In addition, a series of drugs mimicking the Smac activity are investigated, since this protein binds to the IAP promoting the activation of procaspase 3.
- **Targeting caspases:** caspases can be activated by using specific drugs aimed to caspases activation or by gene therapy.
- **Targeting TRAIL receptors:** as said before, the most important death ligands in the extrinsic pathway are the Tumor Necrosis Factors (TNF). Another death ligand is the TNF-related apoptosis-inducing ligand (TRAIL), whose receptor is a good target for inducing apoptosis.

## 1.4 Aim of the thesis work

The development of new anticancer drugs targeted to tumor cells apoptosis is an important but also a challenging point in cancer research. Usually, drug discovery trials are very expensive processes, since they require human and animal models, and additionally it is very frequent that after all the costly and long clinical trials the drug is not approved. The current efforts in drug discovery are aimed to the creation of reliable *in vitro* models for predicting the toxicity of agents on tumor cells and overcoming the costs and the ethical issues of using human and animal models [8].

The aim of the present work is to introduce a non-invasive, label-free and real-time procedure for analyzing *in vitro* tumor cells behaviour in presence of a drug by simply monitoring modifications in their morphology. This is possible thanks to the implementation of impedance measurements: if a certain number of cells is seeded on a surface made up of metallic electrodes, the analysis of the electrodes coverage degree by cells allows to determine the cells activity. In this perspective, impedance measurements on cell cultures can be an efficient and cost-effective solution in drug screening, cytotoxicity assays and cancer studies [9].

Specifically, in the present work, the impedance measurements were conducted by seeding tumor cells on a CMOS-based chip (BioChip 4096E, *3Brain* GmbH, Switzerland), which

is a multi-electrode array (MEA) probe, i.e. it contains 4096 electrodes at the bottom of a culture chamber: a part of these electrodes is used for impedance readings.

## 1.5 Electric Cell-substrate Impedance Sensing (ECIS)

Before investigating what is Electric Cell-substrate Impedance Sensing (ECIS), it is necessary to introduce some notions about the electric model of cells and the general concept of impedance.

### 1.5.1 Electric model of a cell

As it is known, a cell is delimited by the plasma membrane, a phospholipid bilayer having the functions of separating intra- and extracellular fluids, providing mechanical protection, allowing communication between adjacent cells or between cells and extracellular matrix. Moreover plasma membrane plays a fundamental role in the control of the substances movements from or towards the cell, being selectively permeable to a certain number of ions or molecules: this leads to the creation of ion concentration differences between its intracellular and extracellular domain; for this reason a *membrane potential* is generated across the plasma membrane, ranging from 70 to 90 mV in normal conditions.

Because the cell membrane has the role to prevent the movement of ions, it can be compared to an electrical resistor: the membrane resistance is inversely proportional to the number of ion channels present. Additionally, since an electric potential is established across the membrane, it can also be associated to an electric capacitor. Hence, the equivalent circuit for a single cell is basically a *RC parallel circuit* [10].

### 1.5.2 What is impedance?

If a cell layer is formed above an electrodes array, through the generation of a current between a couple of electrodes it is possible to measure the opposition to the current flow given by the presence of cells, as shown in figure 1.3 [10].

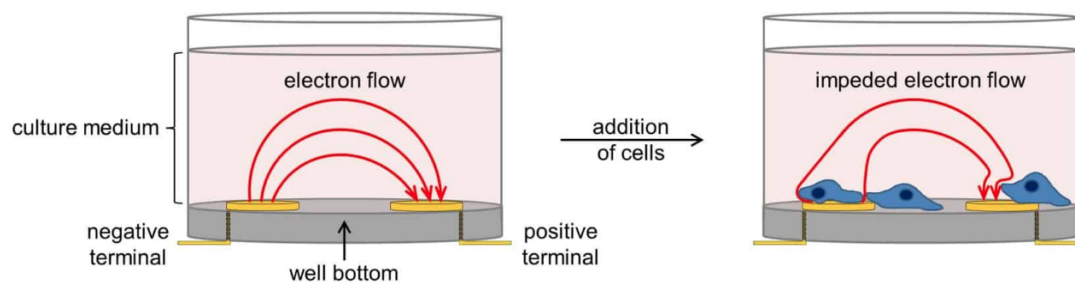


Figure 1.3: Schematic explanation of cells opposition to a current flow. [10]

Obtaining a quantification of cells impedance, characterized by cell resistance ( $R_{\text{Cell}}$ ) and cell capacitance ( $C_{\text{Cell}}$ ) is very important to describe cells behaviour; infact by measuring the opposition of cells to the current flow, it is possible to deduce the cell status on the electrode's surface. For having a precise quantification, it would be reductive and incorrect to conduct a DC measurement, which would provide information only concerning the resistive part of the equivalent circuit, respecting Ohm's Law (equation 1.1). In this specific case a constant current is generated between two electrodes and the opposition to

its passage is represented by resistance ( $R$ ).

$$R = \frac{V}{I} \quad (1.1)$$

It is instead useful to conduct an AC measurement, in order to take into account also the capacitive part of the equivalent circuit. In this case an alternating current (often sinusoidal) is generated between two electrodes and the opposition to its passage is represented by impedance ( $Z$ ) [11].

Impedance is a complex quantity, hence it is composed of two parts:

- a real part, i.e. the resistance ( $R$ ), which does not vary depending on the frequency;
- an imaginary part, called reactance ( $X$ ), whose value is dependent on the frequency and describes the presence of capacitors (capacitive reactance  $X_C$ ) or inductors (inductive reactance  $X_L$ ), taking into account respectively eventual electrostatic energy accumulations or magnetic energy accumulations.

$$X = X_L + X_C = 2\pi fL + \frac{1}{2\pi fC} \quad (1.2)$$

where  $f$  is the frequency,  $L$  is inductance and  $C$  is capacitance.

In mathematical terms impedance is expressed as follows:

$$Z(\omega) = \frac{V(\omega)}{I(\omega)} = \text{Re}(Z) + j\text{Im}(Z) = R + jX(\omega) \quad (1.3)$$

where  $\omega$  is the angular frequency ( $\omega = 2\pi f$ ) and  $j = \sqrt{-1}$ .

Impedance modulus and phase may be calculated as follows (equations 1.4 and 1.5):

$$|Z(\omega)| = \sqrt{R^2 + (X(\omega))^2} \quad (1.4)$$

$$\phi = \arctan\left(\frac{X(\omega)}{R}\right) \quad (1.5)$$

The impedance modulus is the characterizing parameter of the cell status, while phase does not provide significative information [12].

### 1.5.3 How can cell impedance be measured?

There are several methods for measuring cellular impedance, depending on the purpose, even if the basic principle is the same: an AC current flow ( $I_x$ ) is generated between two electrodes and impedance is derived by measuring the voltage ( $V_x$ ) between the electrodes and executing the ratio  $V_x/I_x$ .

If one is interested to conduct cell counting operations, *impedance flow cytometry* (IFC) is employed: this procedure exploits an AC current passing between two electrodes located on the opposite sides of a microchannel, where cells are kept in suspension. Each time a cell passes between the electrodes, the current flow is prevented, hence a peak of impedance is registered. As a result, by counting the impedance peaks, it is possible to trace back to the number of cells passed. IFC is limited to measurements at a single frequency value and it is used when cells are in suspension [9].

Another way for measuring impedance on cells is represented by *electric impedance spectroscopy* (EIS). It is also referred to cells in suspension but, differently from IFC, it employs

a range of frequencies (multi frequency measurement) in order to evaluate the frequency value at which the system's response (current blocking by cells) is maximum: this operation is the so called "frequency sweep". A limitation of this procedure is the time-consuming frequency sweep analysis for long-time monitorings; a simple solution can be implemented by conducting a first measure using the frequency sweep, choosing the maximum response frequency and then employing this value for the successive single frequency analysis [9]. Since this thesis work has the purpose to study impedance on a cell layer which is adherent to the electrodes surface, the measurement method employed is the *electric cell-substrate impedance sensing* (ECIS). This is a technique introduced by Giaever and Keese in 1991 [11], in which cells are grown on an array of electrodes and their adhesion degree is monitored; it is suitable for adherent cells analysis and long-monitoring assays and very precise, thanks to the exploitation of the frequency sweep. Hence, from this point on, all the expressions of impedance measurements will be intended as ECIS measurements.

#### 1.5.4 Parameters influencing cell impedance measurements

Many parameters must be considered to model the cell layer-electrodes interface, reported in figure 1.4 [11].

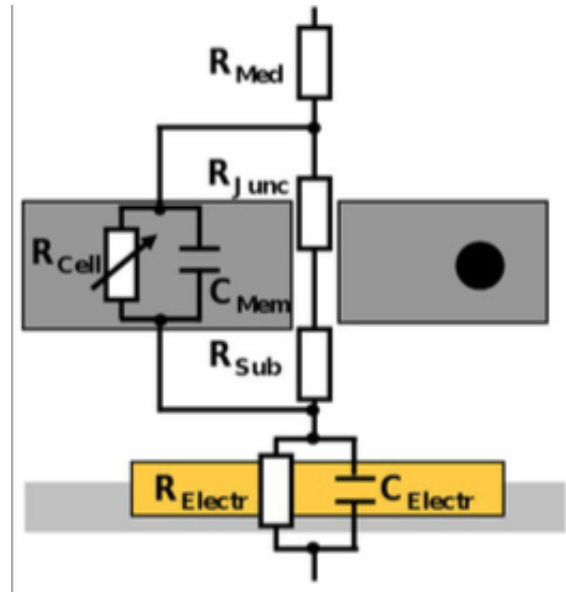


Figure 1.4: **Electric model of a cell layer above an array of electrodes.** The grey bodies represent adjacent cells. In addition to the single cell resistance ( $R_{Cell}$ ) and cell capacitance ( $C_{Cell}$ ), the resistances associated respectively to cell-cell junctions ( $R_{Junc}$ ), to the culture medium ( $R_{Med}$ ), to the space between cells and electrodes ( $R_{Sub}$ ) and the parallel circuit formed by the resistance ( $R_{Electr}$ ) and the capacitance ( $C_{Electr}$ ) of the electrode-electrolyte interface must be considered. [11]

The equivalent circuit involves the following features [11]:

- the RC parallel circuit representing the electric model of a single cell, as described above ( $R_{Cell}$  and  $C_{Cell}$ ). As visible in figure 1.4,  $R_{Cell}$  is variable according to the number of ion channels, which defines cell permeability.  $C_{Cell}$  is related to the phospholipid bilayer properties;
- the resistance associated to the cell-cell junctions ( $R_{Junc}$ );

- the resistance of the culture medium ( $R_{\text{Med}}$ );
- the resistance associated to the space between the cell layer and the electrodes array, index of the cell-substrate adhesion ( $R_{\text{Sub}}$ );
- the RC parallel circuit describing the electric model of the electrode-electrolyte interface ( $R_{\text{Electr}}$  and  $C_{\text{Electr}}$ ).

Although the mentioned additional parameters to  $R_{\text{Cell}}$  and  $C_{\text{Cell}}$  affect impedance measurements, it is possible to tune the stimulation frequency, in order to reduce the effect of the components which are not of interest and focus just on the components related to the cell body, for evaluating the coverage degree of the electrode surface and monitoring cell status. Infact, at low frequencies (less than 10 Hz) the impedance component given by the electrode-electrolyte interface ( $R_{\text{Electr}}$  and  $C_{\text{Electr}}$ ) is predominant; at high frequencies (more than 100 kHz) the resistance of the culture medium ( $R_{\text{Med}}$ ) dominates. By contrast, if frequency is maintained in an intermediate range, the greatest contribute is given by the components related to the cell body [13].

It is important to know that depending on the frequency employed, the cell layer behaviour can vary. At low frequencies (less than 2 kHz) cells reactance increases (being  $X$  inversely proportional to  $f$ ), hence the current has a higher probability to flow between cells, as highlighted in figure 1.5 by the red arrows. At high frequencies (more than 40 kHz) cells reactance decreases, so the current has a higher probability to flow through the cells, as visible in figure 1.6 by the green arrows [14].

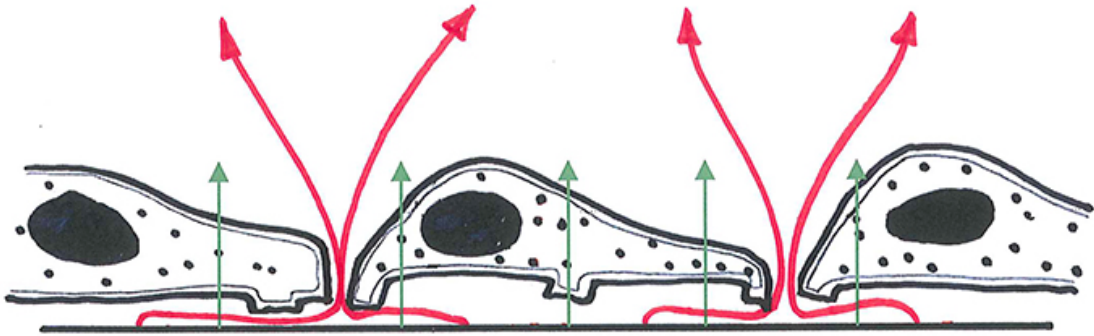


Figure 1.5: **Cells behaviour at low frequencies current (< 2 kHz)**. Since cell reactance increases, the current passes through the junction between adjacent cells. [14]

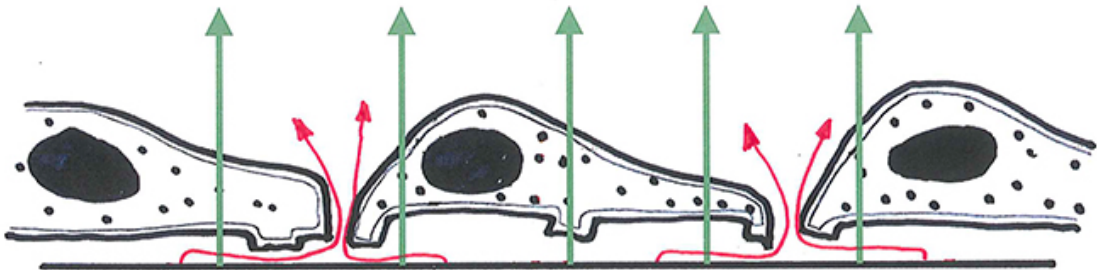


Figure 1.6: **Cells behaviour at high frequencies current (> 40 kHz)**. Since cell reactance decreases, the current passes through the cell body. [14]

In figure 1.7 a schematic representation of cell-electrode interaction is reported. As the cell adheres and spreads over the electrode, the coverage degree increases and consequently impedance increases, since the current flow is more impeded [15].

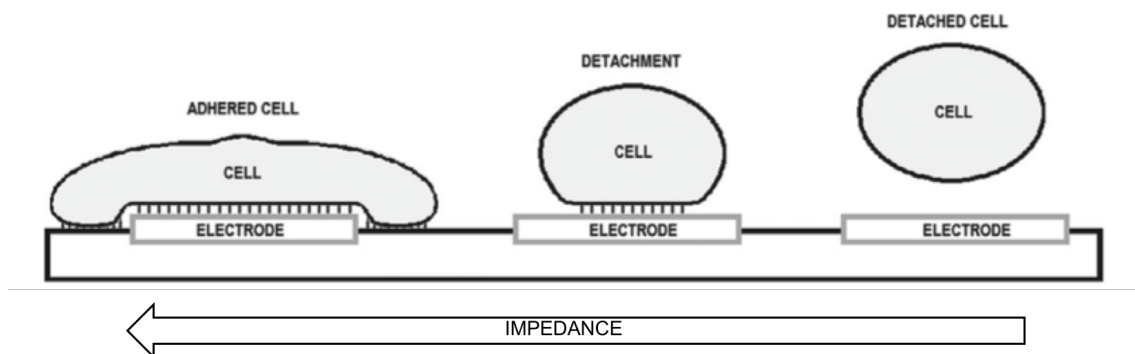


Figure 1.7: **Schematic representation of cell-electrode interaction.** As the electrode's covered area increases, impedance increases. [15]



## Chapter 2

# State of the art

### 2.1 The drug development process

The development process of a drug is a long and expensive process: averagely, at least 10 years are necessary for a drug to be put on the market and the costs associated to the trials are about \$ 2,6 billions [16]. The drug development process is composed of three phases [17]:

1. **Drug discovery:** it is a preliminar process, in which researchers start either from the disease or from the new compound; in the first case, a compound producing positive effects against the specific disease is designed. In the second case the effects of a substance are tested over a great number of diseases. Once a promising compound comes out from these analysis, it is ready for the further steps.
2. **Preclinical phase:** it is a phase in which tests *in vitro* and *in vivo* are executed, respectively on cell cultures and on animal models. It is a crucial phase, since the researchers decide if the compounds can be tested on humans.
3. **Clinical phase:** it is conducted on people; before starting, researchers establish how the experiments will be executed, in the so called Investigational New Drug process (IND). The clinical process includes three phases. The first phase lasts several months and is carried out for establishing drug's safety and dosage; 20-100 volunteers or people with diseases are required and 70% of the drugs moves to the next phase. The second phase may last 2 years and is conducted for evaluating drug's efficacy and side effects; several hundreds people with disease are required and 33% of the drugs succed to the next phase. The third phase lasts from 1 to 4 years and is useful for monitoring the side effects; it employs from 1000 to 5000 volunteers with diseases and 25% of the drugs passes to the next phases.

After these phases, if the drug has revealed to be safe, a New Drug Application (NDA) resumes all the data obtained from the previous phases and is examined by FDA (Food and Drug Administration), that decides if the drug may be approved.

If the drug is approved by FDA, it is placed on the market and a post-marketing safety monitoring is started [17].

Figure 2.1 reports some information about the drug development process: the drug discovery and preclinical phases last 3-6 years, the clinical one lasts 6-7 years. After the placing on the market, a post-marketing safety monitoring is executed over an undefined period of time.

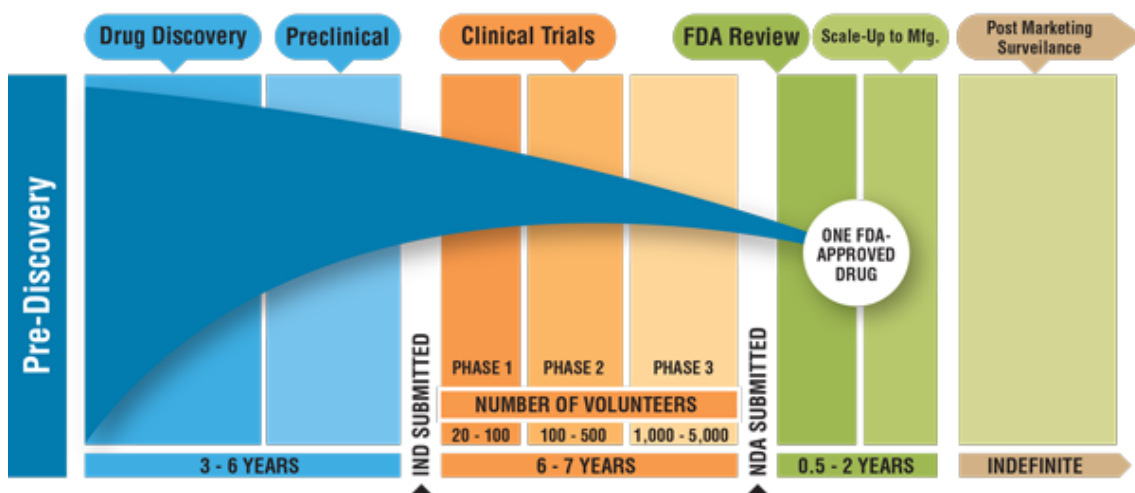


Figure 2.1: **Drug development timeline.** The funnel represents the number of compounds which succeed from one phase to the next; averagely, one compound over several thousands is placed on the market. [16]

There are a series of issues associated to the drug development process. Firstly, once a drug is commercialised, its withdrawing from the market would cost approximatively \$ 800 millions. Additionally, the majority of the tested compounds does not pass from the preclinical phase to the clinical phase, due to the substantial differences between animal models and human models. Furthermore, the experiments on animal models are very expensive and always raise ethical issues: the current ethical trend imposes to Reduce, Refine and Replace animal testing ("3R" concept). For all these reasons, finding reliable systems which predict the toxicity of a new compound in the earliest steps of the drug development would strongly reduce the costs in terms of money and time for drug discovery [18][19].

## 2.2 Current drug screening tests

Nowadays the number of chemical compounds as candidates to become FDA-approved drugs is huge. This aspect would require an increase of test cases in animal experimentation, economically and ethically unprofitable. For this reason today there is a need to improve the reliability of *in vitro* models in order to reproduce as well as possible the human *in vivo* environment, for conducting precise and cost-effective toxicity studies [18]. The most diffused *in vitro* models are 2D cell cultures, due to their numerous advantages:

- facility of the culture maintenance;
- lower costs than animal models;
- great availability of the instruments and equipment for the culture maintenance;
- possibility of conducting high throughput screening (HTS) assays, thanks to the use of multi-well plates instead of single culture dishes.

Even the 3D cell cultures, firstly introduced in the field of tissue engineering, are becoming a good platform for toxicity studies, since they allow to more accurately replicate the 3D microenvironment of a disease [18].

The most common *in vitro* assays for assessing drug toxicity are reported in table 2.1:

Table 2.1: Principal drug cytotoxicity assays. [18]

Assay	Purpose	Advantages	Disadvantages
MTT, XTT, MTS assays	Used for evaluating the metabolic activity of cells and proliferation	Easy to execute	Unable to distinguish between cells necrosis and apoptosis
Alamar Blue	Cells proliferation assessment	Easy to execute	Unable to distinguish between cells necrosis and apoptosis; weakly sensitive
CellTiterGlow	Measurement of energy (ATP) depletion by cells	Easy to execute	Unable to distinguish between cells necrosis and apoptosis
ToxiLight	Measurement of cytolysis; more indicated for necrosis assessment	Not destructive	Higher drug doses required
Lactate dehydrogenase (LDH) assay	Measurement of cytolysis; more indicated for necrosis assessment	Not destructive	Higher drug doses required

As visible from table 2.1, there are many assays to test the cytotoxicity of a compound, each of which investigates different mechanisms, such as cell proliferation, cytolysis, etc.. In particular, apoptosis can be evaluated through the MTT assay; this assay uses 3-(4,5-dimethylthiazol-2-yl)-2,5-diphenyltetrazolium bromide (MTT), a compound which becomes fluorescent when it is reduced by intracellular enzymes to formazan, acquiring a blue fluorescence. This occurs only in living cells, when the enzymes are activated. Hence, the fluorescence degree is index of cell viability. Once stained, the cell culture must be analysed through fluorescence microscopy. Other assays to assess cellular apoptosis are the TUNEL assay and the Annexin V assay, which will be explained in detail later.

However, the typical issues of using the classic laboratory assays are related to the high costs of the reagents, kits and instrumentation. Moreover, as visible from table 2.1, most of the drug toxicity assays present disadvantages, such as their inability to discriminate between cells apoptosis and necrosis. Hence, research is focused on new cost-effective and label-free methods for screening procedures [20].

An emerging platform for drug discovery is represented by the organs-on-a-chip, microscale devices whose fabrication techniques result from the semiconductors industry. An organ-on-a-chip platform is obtained when cells are seeded onto a microfluidic device. In such a system the cell culture is controlled in many ways and the presence of microchannels allows the perfusion of liquids: a dynamic condition for toxicity studies can be created. To better replicate the *in vivo* condition, different types of cells can be seeded, in order to mimic the cellular phenotype heterogeneity typical of human tissues and diseases [8].

## 2.3 Platforms for drug screening tests by impedance measurements

Another disadvantage of the *in vitro* drug toxicity assays is their inability to provide real-time information: the results of a classic toxicity assay are referred only to the time point investigated. Hence, currently, researchers are looking for methods providing real-time information about the evolution of a cell culture [19].

As explained before, the aim of this thesis work is to provide an effective method to monitor cell status over time in presence of a drug. The platform consists of a chip, fabricated through the cost-effective CMOS (Complementary Metal-Oxide semiconductor) techniques and able to read impedance changes due to cells attachment thanks to the presence of metallic electrodes integrated in the system.

Figure 2.2 reports the typical architecture of a microelectrode.

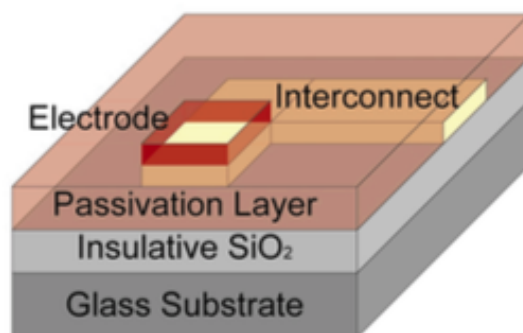


Figure 2.2: Materials and architecture of each microelectrode in a CMOS-based MEA (multi electrode array). [21]

The cell-substrate impedance measurement method is:

- label-free, because cells do not need to be marked in any way. The information provided is simply dependent on the cell shape on the electrode, index of cell status;
- non-invasive, since just an electrical parameter (impedance) is considered for cell analysis and does not disturb the cell cycle;
- real-time, because the cell culture can be monitored over time, due to the fact that this method is non-destructive.

For these reasons this is a promising procedure for drug discovery studies: through a simple measurement of an electrical parameter as impedance, it is possible to obtain more information than the previously listed assays, without labelling cells and saving time and costs [19].

In the last years, a series of devices have been proposed for implementing impedance measurements on a cell culture, with different aims.

Specifically, with regard to impedance measurements for drug screening studies, a homemade system design can be obtained by seeding cells on a cell culture dish; at the bottom of the well a certain number of gold microelectrodes are placed, in order to measure impedance changes reflecting cells adhesion, proliferation and apoptosis [12][22]. Moreover,

other commercial devices integrating microelectrodes at the bottom of the culture chamber can be found [20][23][24]. A famous commercial example is the xCELLigence® RTCA instrument (Roche), capable of conducting a prolonged real-time analysis of the cell culture providing information about different phases of the cell cycle. Its design is reported in figure 2.3: the system can integrate six 96-well electronic plates (E-Plate® 96), which can be independently controlled. The instrument is placed in an incubator 5%  $CO_2$  and communicates with a dedicated software [10].



Figure 2.3: **xCELLigence® system design**. Six 96-well plates can be monitored at the same time; the parameters are set through the dedicated User Interface. [10]

Figure 2.4 reports the expected impedance curve from the xCELLigence® analysis [10]. This system does not plot the  $|Z|$  value, but a normalized value, called Cell Index (CI), obtained from the ratio of each measured value at time  $t$  and the impedance value at time 0 [19].

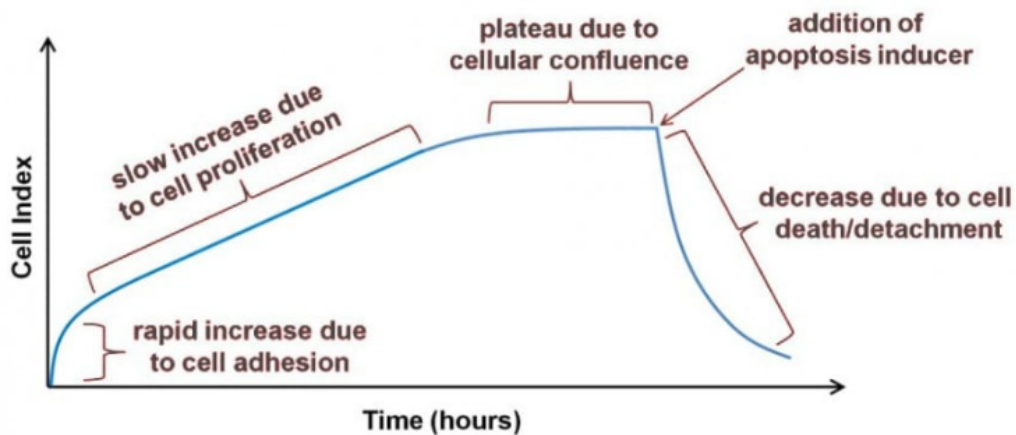


Figure 2.4: **Expected impedance curve from xCELLigence® system**. The system can provide information about several cells activities, i.e. adhesion, proliferation and death in presence of a toxic agent. [10]

The advantages and disadvantages of the impedance measurement method compared to the MTT assay, which is one of the most diffused cell viability assays in drug screening, are resumed in table 2.2 [12][25].

Table 2.2: Advantages and disadvantages of ECIS compared to the MTT assay. [12][25]

<b>Assay</b>	<b>Advantages</b>	<b>Disadvantages</b>
<b>MTT assay</b>	<ul style="list-style-type: none"> <li>• Not expensive</li> <li>• Easy to execute</li> <li>• Good sensitivity</li> </ul>	<ul style="list-style-type: none"> <li>• Information related to a single time point</li> <li>• Requires labelling</li> <li>• For prolonged exposures, the label is toxic</li> <li>• Unable to distinguish between cells necrosis and apoptosis</li> </ul>
<b>ECIS technique</b>	<ul style="list-style-type: none"> <li>• Real-time</li> <li>• Label-free</li> <li>• Non invasive</li> <li>• Not expensive</li> <li>• Easy to execute</li> </ul>	<ul style="list-style-type: none"> <li>• Not extendable to 3D cultures</li> <li>• Unable to distinguish between cells necrosis and apoptosis</li> <li>• Sensitivity must be improved</li> </ul>

## Chapter 3

# Experimental set-up

Although the purpose of this thesis is evaluating the impedance changes in cell culture induced by the presence of a toxic agent for drug screening applications, some preliminary steps were necessary, for ensuring viability and proliferation of cells once seeded on an electrodes area. For this reason, the work carried out can be schematically divided into two phases:

1. Set-up of optimal conditions for cell adhesion and growth on the BioChip;
2. Evaluation of apoptosis following drug administration.

Both steps were conducted by monitoring impedance changes over time.

In this chapter, the equipment employed for the impedance measures is described and the experimental procedures used to conduct the measurements are explained. The schematic representation of the experimental set-up is reported in figure 3.1.

Briefly, a commercial chip named BioChip 4096E (*3Brain GmbH*, Switzerland), exhibiting a culture chamber, is seeded with the cell line to be submitted to the impedance measurements. A PC communicates via GPIB with a precision impedance analyzer (*Agilent 4294A*), in order to command the instrument directly from a Graphical User Interface created in LabVIEW® 2017 (*National Instruments Corp.*). The PC is also connected via USB to a breadboard where an Arduino® Micro and two CMOS analog multiplexers (*CD4067*, *Harris® Semiconductors*) are present: this platform allows the user to choose a couple of electrodes for conducting the impedance measurements between 16 available electrodes at the bottom of the BioChip's culture chamber. Also this setting is involved in the LabVIEW® interface. Through a program expressly created on the Arduino IDE, the Arduino® allows to activate the desired channels of the multiplexers which are connected to the electrodes pads of the chip through a flat cable. The test fixtures of the impedance analyzer are then connected to the output pins of the multiplexers for the measurements.

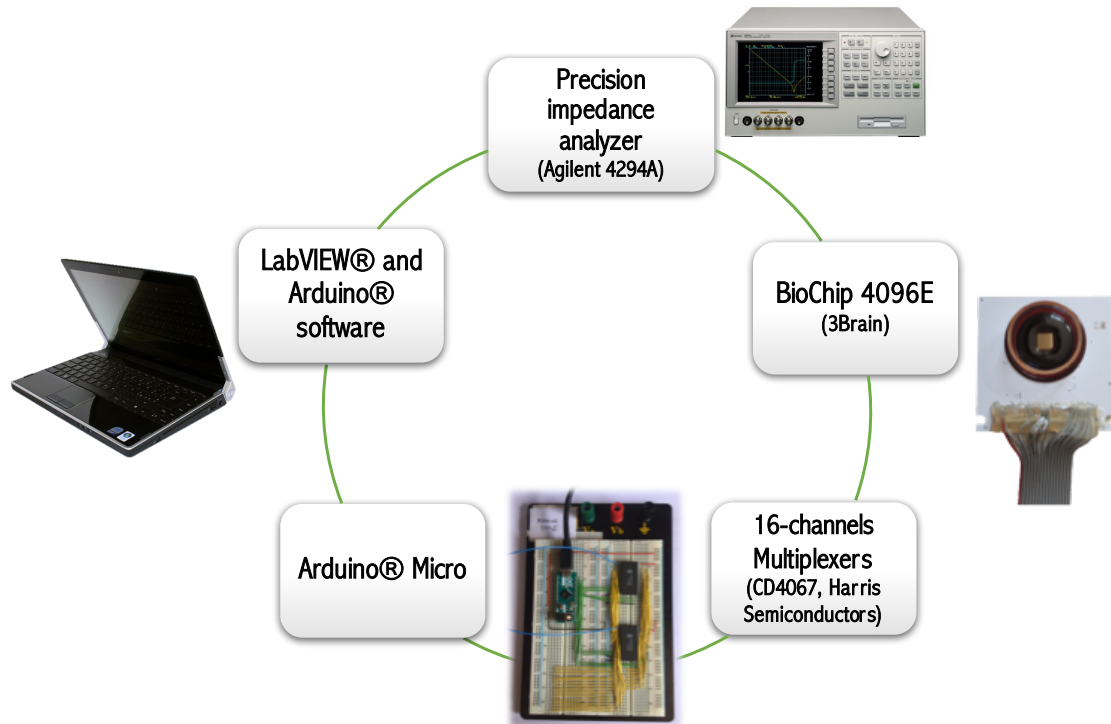


Figure 3.1: Scheme reporting the experimental set-up for the automated impedance measurements.

## 3.1 *3Brain* BioChip 4096E

### 3.1.1 General features

With the aim of measuring impedance, cells must be seeded on an electrodes array. For this purpose, in the present work a commercial chip, BioChip 4096E, was chosen. It belongs to the HD MEA Probes (high definition multi electrode arrays probes) products, which have different features, but in general they have in common 4096 recording electrodes, surrounded by a glass ring suitable to cells seeding and growth. HD MEA Probes are fabricated exploiting CMOS-technology typical processes, which are known to be cost-effective and to reach high resolutions. Thanks to these processes it is possible to integrate such a great number of electrodes on a reduced area. For ensuring biocompatibility, electrodes are coated with platinum.

The BioChip 4096E consists of a printed circuit board (PCB) which integrates contact pads for electrodes connections, a culture chamber and 4096 recording electrodes (64 x 64 matrix) arranged at the center of the chamber delimited by the glass ring, occupying a 5,12 mm x 5,12 mm area. The electrodes dimensions are very small: they have a square geometry with side 21  $\mu\text{m}$  and are equally spaced (81  $\mu\text{m}$  pitch). Differently from the other types of HD MEA Probes, BioChip 4096E also integrates 16 stimulation electrodes (4 x 4 matrix); for this reason it is defined HD-MEA *Stimulo*. Stimulation electrodes have the same size of recording electrodes, but they are spaced 1,3 mm each other, occupying a total area of 3,96 mm x 3,96 mm. All the dimensions of BioChip 4096E are resumed in table 3.1, the general design of the device is presented in figure 3.2 and the electrodes arrangement scheme is reported in figure 3.3 [26][27].

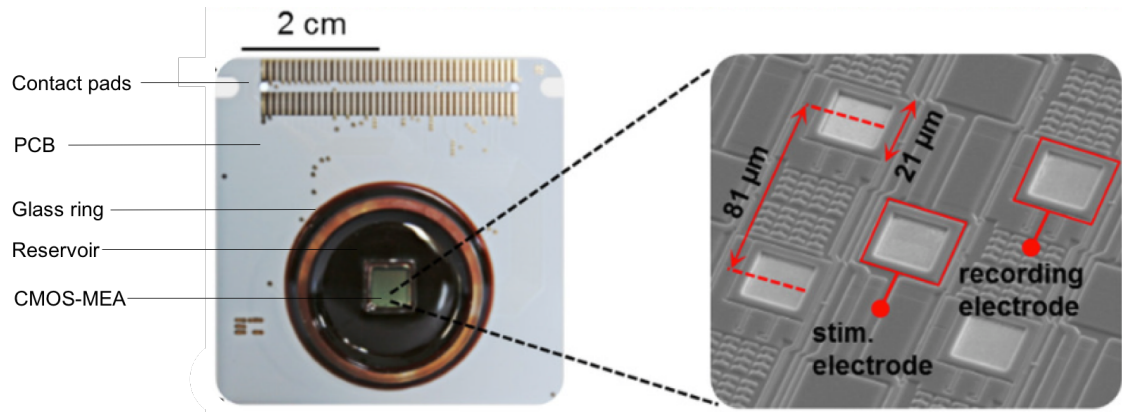


Figure 3.2: Design of BioChip 4096E (3Brain). [26]

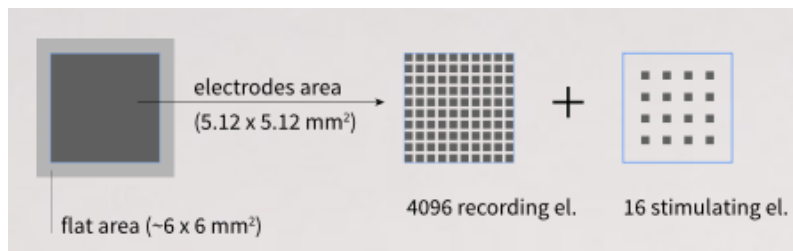


Figure 3.3: Schematic representation of recording and stimulation electrodes arrangement on the chamber's flat area. [27]

Table 3.1: Resuming table of all the dimensions of BioChip 4096E. [27]

	<b>Dimension</b>
PCB size (side)	54 mm
External glass ring diameter	28 mm
Internal glass ring diameter	25 mm
Glass ring height	5 mm
Reservoir capacity	2 mL
Recording area	5.12 mm x 5.12 mm
Stimulation area	3.96 mm x 3.96 mm
Electrode size (side)	21 $\mu\text{m}$
Recording electrode pitch	81 $\mu\text{m}$
Stimulation electrode pitch	1.3 mm

Originally, HD MEA Probes were designed to host cells possessing an electric activity, mainly neurons, in order to measure spontaneous or evoked potential activities with a very high resolution. The great number of electrodes has the aim of augmenting the statistical significance of the measures; moreover, by conceiving each electrode as a pixel, the final result is a precise mapping of neurons electrophysiology over the electrodes area, as an image. Each recording electrode incorporates a system of amplifiers and filters, in order to conduct the signal processing directly in contact with cells, where the signal is prelevated. This aspect strongly increases the signal to noise ratio [27].

The presence of stimulation electrodes, which do not have all the circuitry for the signal processing and can be used as simple reading electrodes, allows to extend the use of the BioChip *Stimulo* to many fields and to seed and grow several kinds of cell lines different from neurons, in order to conduct other types of analysis. Specifically, for this thesis purpose HT-29 cells were used, optimizing the culture protocol (established for neurons) [26] for this cell line and exploiting the stimulation electrodes for impedance measurements. Figure 3.4 shows the electrodes array morphology with a cell adhered on the surface of a microelectrode [28].

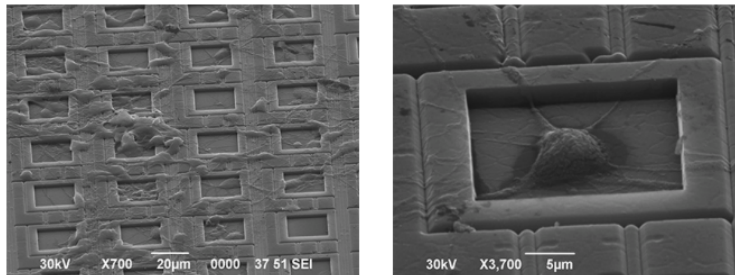


Figure 3.4: **Scanning electron microscopy (SEM) image showing the electrodes morphology.** A cell adhered on the electrodes surface can be seen. [28]

### 3.1.2 BioChip 4096E sterilization and cleaning protocols

Before starting to use the BioChip 4096E, it is necessary to strictly follow a protocol to ensure its cleanliness and sterility. Using autoclave or UV light, touching the active area and keeping the culture medium pH in a different range from the physiological one (7-7.5) could be fatal for the electrodes working. Hence, handling the chip with care before and during the use is very important for the success of the measurements. The sterilization steps before using the BioChip are realized under laminar flow hood and are listed as follows [29]:

1. If the chip has been kept in a dry environment for a long time before its use, it is advisable to fill the chamber with double distilled water (DDW) for 1-2 hours;
2. The entire chip is cleaned with paper soaked in ethanol 96%;
3. The chamber is filled with ethanol 70% for 20 minutes;
4. The chamber is washed 5 times with DDW, to eliminate the residual ethanol;
5. After withdrawing water, the chamber is let to dry under laminar flow.

After the use, the BioChip must be cleaned; the procedure used for the present work is here reported:

1. The culture medium is aspirated;
2. The chamber is bountifully washed with DDW;
3. The chamber is filled with ethanol 70% for 5 minutes;
4. A soft brush is used to remove the residual cells;
5. The chamber is again washed 5 times with DDW, to eliminate the residual ethanol.

When the cleaning procedure is completed, the BioChip can be stored.

## 3.2 HT-29 cell line

### 3.2.1 General features

The cell line used in the present work is the HT-29 cell line (ATCC® HTB-38™), from human colorectal adenocarcinoma, kindly provided by Dr. Danny Incarnato. The features of this cell line are listed in table 3.2 [30]. HT-29 are widely used in many studies. They can express, if treated under specific conditions, different aspects of the enterocytes differentiation; for this reason they are recognized as pluripotent intestinal cells and studied for monitoring the immune intestinal response to infections. Moreover, HT-29 cells are a very robust cell line for *in vitro* cultures: this allows to assess their behaviour under the action of a certain number of anticancer agents [31].

Table 3.2: HT-29 cell line features. [30]

<b>Organism</b>	<i>Homo sapiens</i> , human
<b>Tissue</b>	colon
<b>Disease</b>	colorectal adenocarcinoma
<b>Age</b>	44 years
<b>Gender</b>	female
<b>Ethnicity</b>	caucasian
<b>Morphology</b>	epithelial
<b>Growth properties</b>	adherent
<b>Shipped</b>	frozen
<b>Storage</b>	liquid nitrogen
<b>Population doubling time</b>	23 hours
<b>Recommended subculturing ratio</b>	1:3 to 1:8
<b>Medium renewal per week</b>	2-3 times

For the purpose of this thesis, since a 2D culture is needed to conduct ECIS, HT-29 cells were chosen because they are anchorage-dependent and have the tendency to form adherent monolayers with tight junctions. They are shipped in a frozen state (dry ice) and when removed from their packaging, they are placed in liquid nitrogen vapor until their use (cryopreservation at -180°C), in order to avoid a loss of viability. Hence, before obtaining a cell culture, HT-29 cells must be thawed. After thawing, a certain period of time is necessary for cells to recover their activity. Once thawed, cells can be kept for several days in culture, incubated at 37°C, 5% CO<sub>2</sub>. In general cells growth in culture follows three phases: immediately after seeding there is a *lag phase*, in which cells start

growing slowly. Then a *log phase* occurs, in which cells proliferate exponentially. This phase is followed by a *stationary phase*, in which cells stop proliferating either because the culture medium nutrients are exhausted or because cells have reached the maximum confluence, i.e. they have occupied all the available area. In general, after the achievement of the stationary phase, cells start to lose viability. The typical growth curve for cultured cells is reported in figure 3.5. For preventing that the stationary phase is reached and ensuring the maintenance of the cell culture during time, cells must be subcultured: the subculturing (or passaging) process consists in the detachment of cells from the culture dish and in their splitting in a defined number of new culture dishes, with a supplement of fresh medium. The periodicity of the subculturing is dependent on the cell type, density and culture area [32].

When a large population of cells is obtained, a part of them can be again frozen, in order to have a stock for the eventuality of additional experiments.

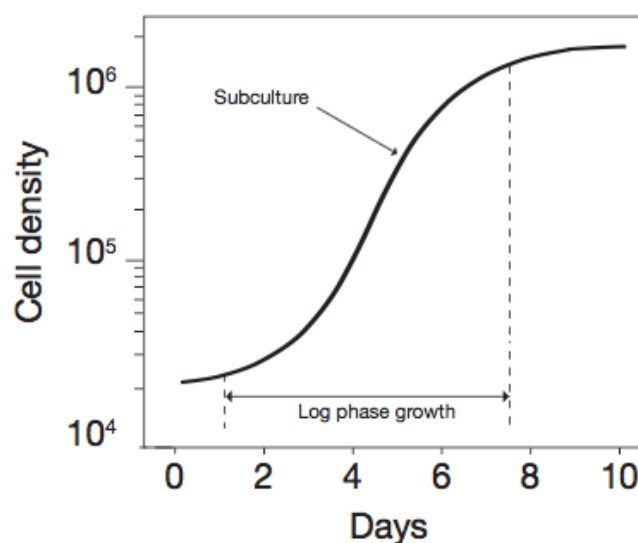


Figure 3.5: **Growth curve for cultured cells.** Initially a slow growth (lag phase) is verified; then an exponential growth phase occurs (log phase) and it terminates when a plateau is reached (stationary phase), indicating that cells are not proliferating anymore. The correct moment for subculturing cells is indicated in figure. [32]

As HT-29 are adherent cells, they stop proliferating if they occupy the total area available (100% confluence). Hence, in general HT-29 are subcultured in the *log phase*, when they reach 80-90% confluence.

Depending on the cell line, it is very important to choose the appropriate culture medium, which contains nutrients, hormones and growth factors for cells growth and additionally it regulates the culture's pH (7.4 for mammalian cells) and osmotic pressure [32]. In this case the culture medium used is composed of three elements:

- RPMI 1640 (EuroClone®) with L-Glutamine; HT-29 cell line has a high glucose consumption, hence a high glucose concentration is required.
- 20% FBS (fetal bovine serum, Gibco™ by *Life Technologies*), which is a source of growth factors and hormones for cells growth.
- 1% PS (Penicillin-Streptomycin, Gibco™ by *Life Technologies*), an antibiotic solution for preventing bacterial contamination.

The culture medium is prepared using a Corning® Bottle-Top Vacuum Filter System (*Sigma*) equipped with a 0,22  $\mu\text{m}$  filter and a cap for storage. The solution obtained from the previously listed elements is prepared in the top part of the filtering system and by creating the vacuum, it is filtered and collected in the bottom part of the system, which is a bottle and is closed with its cap for being stored at 4°C until use. Figure 3.6 reports the culture medium preparation phase, under laminar-flow hood.

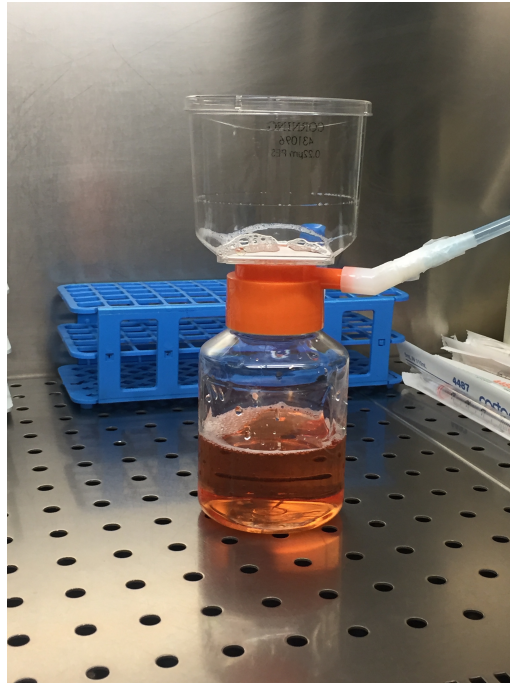


Figure 3.6: **Preparation of the culture medium through a Corning® Bottle-Top Vacuum Filter System (*Sigma*).**

In the following sections, the thawing, freezing and subculturing protocols for HT-29 cell line are reported. All procedures are conducted under a laminar flow hood for maintaining sterility.

### 3.2.2 Thawing protocol

The steps executed for the thawing procedure in the present work must be conducted very fastly and are reported as follows [33]:

1. Cells are prelevated from liquid nitrogen.
2. The vial containing cells is thawed by hand or in a 37°C water bath for 2 minutes. It is important to conduct all the following steps under laminar-flow hood.
3. 0,5 mL of fresh culture medium are added to the vial.
4. Cells suspended in culture medium are transferred into a 15 mL falcon containing 4,5 mL of medium.
5. The tube is centrifuged at 1000 rpm for 5 minutes; meanwhile a culture dish (Corning®, 100mm x 2mm) is labelled.
6. Once centrifugation is terminated, the medium is aspirated, taking care not to aspirate also the cells pellet.

7. Cells are resuspended in 4 mL of fresh medium and transferred to the culture dish containing 4 mL of medium, in order to reach a final volume of 8 mL.
8. The culture dish is softly agitated to allow a uniform distribution of cells.

After thawing, the cell culture was maintained alive for the successive experiments by submitting it to periodical subcultures and medium renewals.

### 3.2.3 Freezing protocol

The steps of the freezing protocol are reported below [33]:

1. The culture medium is aspirated from the culture dish.
2. The culture dish is washed twice with 5 mL of PBS (phosphate buffered saline).
3. 0,5 mL of trypsin (Gibco™ by *Life Technologies*) are used to detach cells from the culture dish.
4. The culture dish is kept in incubation for a maximum of 3 minutes, to facilitate the detaching action of trypsin.
5. 5 mL of fresh medium are added to deactivate trypsin (a prolonged trypsin action can result in a loss of cells viability).
6. The content of the culture dish is transferred into a 15 mL falcon and centrifuged at 1000 rpm for 5 minutes.
7. Meanwhile a cryotube is labelled and filled with 0,5 mL of freezing medium (80% FBS, 20% DMSO from *Sigma*, filtered).
8. Once centrifugation is terminated, the medium is aspirated, taking care not to aspirate the cells deposited on the bottom.
9. 0,5 mL of culture medium are added to the cells pellet, well resuspending.
10. The solution is transferred into the cryotube containing the freezing medium, well agitating.
11. The cryotube needs to be put fastly on ice and subsequently at -80°C.
12. If the cryotube must not be used for prolonged periods it is transferred in liquid nitrogen (-180°C).

### 3.2.4 Subculturing protocol

Even in this protocol it is important to conduct all the steps under laminar-flow hood [33].

1. The culture medium is aspirated from the culture dish.
2. The cell culture is washed twice with 5 mL of PBS (phosphate buffered saline), a balanced salt solution.
3. 0,5 mL of trypsin (Gibco™ by *Life Technologies*) are used to detach cells from the culture dish.

4. The culture dish is kept in incubation for a maximum of 3 minutes, to facilitate the detaching action of trypsin.
5. Depending on the number of new culture dishes in which cells must be passaged a certain quantity of medium is added to the trypsin-treated dish for stopping trypsin action. For instance, supposing that a 1:5 passage is required, 4,5 mL of fresh medium are added, obtaining a final volume of 5 mL (since 0,5 mL of trypsin are already present in the culture dish).
6. The new culture dishes (in this case 5 dishes) are labelled and filled each one with 7 mL of fresh medium.
7. Cells in the old culture dish are well resuspended in the fresh medium.
8. 1 mL of cells suspension is added in each new culture dish, obtaining for each one a final volume of 8 mL.
9. The new culture dishes are stacked and gently agitated to allow the cells movement, obtaining a uniform distribution.

### 3.3 HT-29 cell culture protocol on BioChip 4096E

The chip's preparation and culture protocols were made taking a cue from the protocols already established for neurons cultures [26][29], but they were modified to be adapted to the HT-29 cell line. The steps conducted for seeding cells on the BioChip are listed hereunder:

1. **Preconditioning phase:** after sterilization, the chip's chamber was filled with 2 mL of culture medium under laminar hood and the device was kept in incubation (37°C, 5% CO<sub>2</sub>, saturated humidity). For preserving sterility and avoiding the medium evaporation, the chip was positioned into a closed plastic Petri dish (150mm x 15mm). To keep this environment humid enough, an open smaller plastic cell culture dish (35mm x 10mm) filled with DDW was added next to the BioChip (figure 3.7). To prevent possible inclinations of the chip, the soldered flat cable was well fixed to the Petri dish with adhesive tape. The preconditioning phase lasts 48 hours.
2. **Washing:** after the preconditioning, the culture medium was aspirated and the chip's chamber was washed 3 times with PBS.
3. **Chip's coating:** according to the existing protocols, the active area of the BioChip 4096E needs to be coated with an adhesion promoter for cells. In this specific case, collagen type I (C7661 from rat tail, *Sigma*) soluble in 0.1 M acetic acid at 1 mg/mL was chosen. Preliminarily a 50 mL sterile stock solution of collagen in acetic acid (acetic acid glacial, *AnalaR NORMAPUR® ACS*) was prepared at 1 mg/mL. Then a dilution 1:100 (10  $\mu$ L/mL) in PBS was necessary. Since the capacity of the chip's chamber is about 2 mL, 20  $\mu$ L from the stock solution were diluted in 2 mL of PBS. At the end the chamber was filled with the diluted solution and the system was kept at 4°C overnight.
4. **Washing:** the chip's chamber was washed 5 times with PBS.

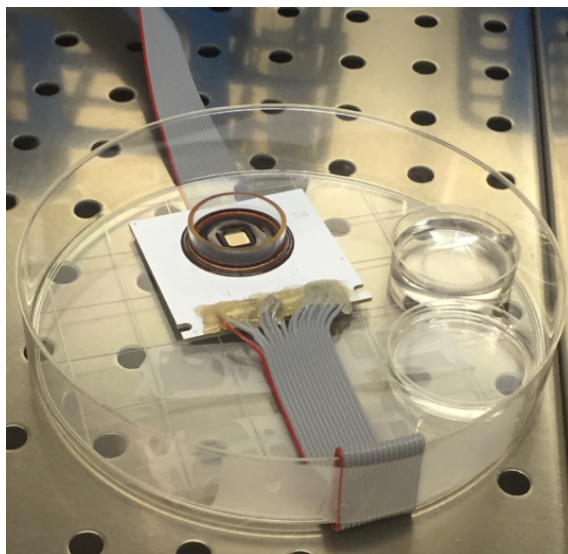


Figure 3.7: **Chip's accomodation for preconditioning phase.** The BioChip 4096E is placed into the big Petri dish, which is closed, together with the smaller cell culture dishes, filled with DDW to preserve humidity. Then the chamber is filled with culture medium and the system is incubated for 48 hours.

5. **Cells seeding:** a small quantity of cells ( $\sim 500$  cells/ $\mu L$ ) must be seeded on the active area of the chip, which is very limited ( $36$  mm<sup>2</sup>). For the seeding procedure cells were prelevated from the Petri dish (100mm x 20mm) where they were seeded and grown after thawing. Cells were detached, resuspended in fresh culture medium and enumerated by using a Countess™ automated cell counter (*Invitrogen*); then they were diluted in a certain quantity of culture medium to obtain the concentration 500 cells/ $\mu L$  and then a 90  $\mu L$  drop was seeded on the electrodes area: approximately 50000 cells were seeded on the chip. To facilitate cell adhesion, laminin (L2020, *Sigma*) was added to the cells suspension with a concentration 10  $\mu g/mL$ . The whole seeding procedure was made under laminar hood, then the chip was incubated.
6. **Culture medium addition:** after 6 hours 1,5 mL of fresh culture medium was added to the chamber and the system was again incubated at 37°C and 5%  $CO_2$ .

### 3.4 Apoptosis inducer: Etoposide

Etoposide (ETO) was kindly gifted by Dr. Federica Fusella and used in the present work, to evaluate eventual changes in cell-substrate impedance in case of apoptosis occurrence. Etoposide is one of the main anticancer agents, being targeted to impede cellular replication, and it is defined as a "broad-spectrum" drug, i.e. it causes apoptosis in a large variety of cell lines. Its target is represented by topoisomerase  $II\alpha$ , an enzyme playing fundamental role in DNA replication.

During DNA replication, topoisomerase  $II\alpha$  cuts DNA double strand in some points and binds covalently to the generated extremities, in order to preserve the integrity of the DNA genetic information, forming a transient *cleavage complex* (enzyme-DNA complex); then it reconnects the DNA double strand. This is done for preventing the supercoiling of DNA [34].

The molecular mechanisms involved in the action of ETO on Topo  $II\alpha$  are still not totally clear, but it is recognized that there are two families of anticancer drugs targeted to topoisomerase  $II\alpha$ : Topo  $II\alpha$  poisons, aimed to stabilize the cleavage complex, and Topo  $II\alpha$

inhibitors, which have an effect on Topo  $II\alpha$  but do not stabilize the cleavage complex [35]. ETO belongs to the family of topoisomerase  $II\alpha$  poisons, in the sense that it links to the cleavage complex, creating a ternary Topo II-drug-DNA complex, which becomes more stable; hence, the number of covalent cleavage complexes augments: these complexes in low quantities are tolerated by the cell, but at high concentrations they produces permanent DNA damages. In this way, double strand breaks are no longer reassembled and their number increases, causing a DNA fragmentation and consequently the cell cycle arrest: cells cannot replicate and the programmed cells death (apoptosis) occurs [36][37].

Etoposide has a terminal half-life of 6 to 12 hours. Since it acts by arresting cells replication, it should be administered to the cell culture during the exponential growth phase, i.e. when cells are proliferating, and not in the stationary phase as for many other drugs. A disadvantage of Etoposide, as for all the anticancer drugs targeted to the DNA, is its low specificity: since it interferes with cells proliferation, also healthy cells may be affected by the drug, especially those cells which multiply rapidly (blood cells or hair cells) [34].

In the present work, ETO was administered to the cell culture after 20 hours from seeding and different concentrations ( $0 \mu M$ ,  $10 \mu M$ ,  $20 \mu M$ ,  $40 \mu M$ ) were tested, to evaluate by the impedance curves a dose-dependent effect on cells apoptosis. After 24 hours of treatment, it was removed by changing the culture medium and the cell culture was monitored for other 36 hours [34].

### 3.5 Agilent 4294A Precision Impedance Analyzer

The instrument used in the present work for impedance measurements is the Agilent 4294A Precision Impedance Analyzer. This device allows the measurement of impedance providing information about different parameters, such as modulus/phase ( $|Z|-\theta$ ) or reactance/resistance (X-R) or many others.

The 4294A performs measures in a frequency range from 40 Hz to 110 MHz (with resolution of 1 mHz) and the test signal may be a current (with resolution of  $20 \mu A$ ) or a voltage (with resolution of 1 mV).

The working principle of the 4294A is shown in figure 3.8. Basically, a voltage is generated as test signal and the current flowing through the device under test (DUT) is measured by an ammeter. The voltmeter measures the voltage generated. Then, the impedance value is obtained from the  $\frac{V}{I}$  ratio [38].

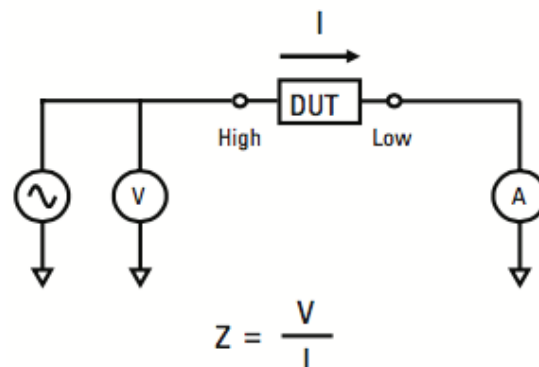


Figure 3.8: **Electric model for impedance measurements by 4294A impedance analyzer.** The device under test is connected to the high and low terminals of the instrument and the impedance value is obtained from the ratio between the generated voltage and the measured current. [38]

The 4294A is suitable to perform sweep analysis, in particular it is possible to conduct a frequency, voltage or current sweep and three sweep modes are available: linear, logarithmic and list sweep. The sweep can be executed from low values to high values ("up") or inversely ("down"). Additionally the number of measurement points can be set and can vary from 2 to 801. Concerning the measurement time, an important parameter to set is represented by the bandwidth, which defines the speed (and consequently the precision) of the measure. Bandwidth ranges from 1 to 5: a value "1" implies a high speed but a low precision, a value "5" implies instead a low speed but a better precision. Moreover the trigger to start a measurement can be sent from an internal source or from an external source and it is possible to send a single trigger or a certain number of triggers and average them, obtaining at the end of the measure the mean curve.

Choosing voltage as test signal, the accuracy can be calculated using the following formula [38]:

$$1mV + (10 + 0.05 \cdot f)\% \quad (3.1)$$

where  $f$  is the frequency in MHz.

When the instrument is connected to the DUT, a measured value is obtained, which is always different from the real value because of the presence of parasitic components characterizing the test fixtures which connect the instrument to the DUT. As visible in figure 3.9, undesired resistances, capacitances and inductances affect the connections: this produces measurement inaccuracies, which can be more or less important according to the test fixtures configuration [38].

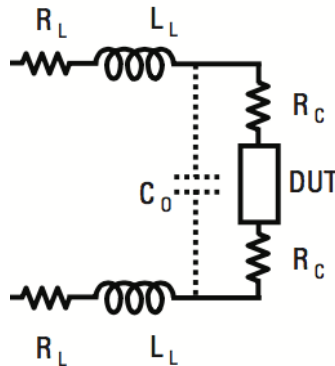


Figure 3.9: **Equivalent circuit of the DUT-fixtures interface.** The test fixture leads are characterized by lead inductances ( $L_L$ ), lead resistances ( $R_L$ ), eventual stray capacitances ( $C_0$ ) and contact resistances ( $R_C$ ). [38]

To resolve this issue, a four-terminal pair configuration (4TP) is used, which reduces all the parasitic contributions, ensuring a high accuracy in an impedance range from 1 m $\Omega$  to 10 M $\Omega$ . The Agilent 16089B Kelvin clip leads, having the 4TP configuration, are the test fixtures used in this work. The front panel of 4294A and the test fixtures design are reported in figure 3.10.

Moreover, a 16-wires flat cable is soldered to the 16 pads of the BioChip 4096E which are referred to the stimulation electrodes and it is employed to extend the length of the connection, since the BioChip must be kept in incubator. By selecting a couple of wires, it is possible to measure impedance between the corresponding BioChip electrodes. When

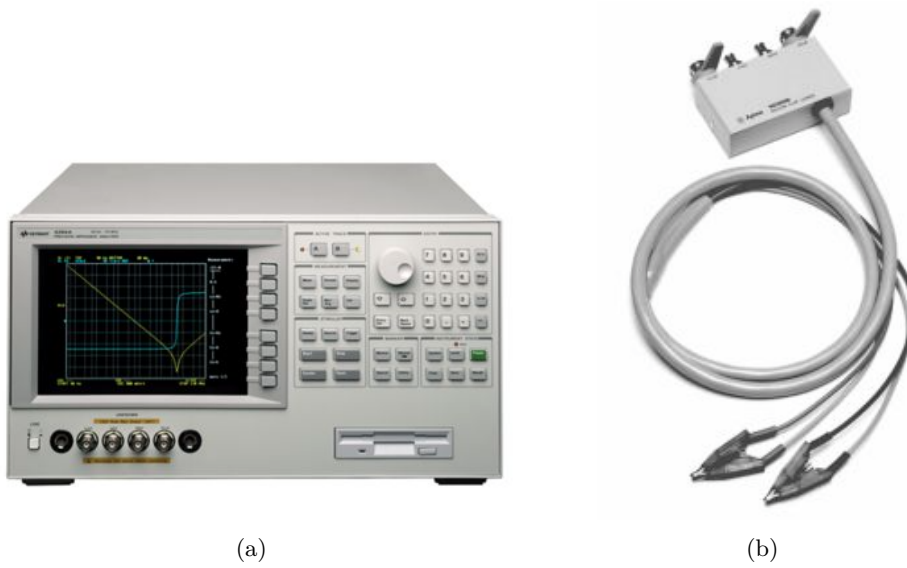


Figure 3.10: a) **Front panel view of 4294A precision impedance analyzer (Agilent) [39]**; b) **Design of the Agilent 16089B Kelvin Clip Leads [40]**.

this cable is used, a relation must be respected for ensuring the maintenance of a high accuracy [38]:

$$L(m) \cdot f(MHz) \leq 15 \quad (3.2)$$

where  $L$  is the cable length and  $f$  is the used frequency for the measurement. Using a maximum frequency value of 1 MHz, this relation would be respected employing a cable length lower than 15 m: in the specific case the flat cable length is about 1,50 m.

Figure 3.11 shows the 16 wires flat cable soldered to the pads correspondent to the stimulation electrodes.

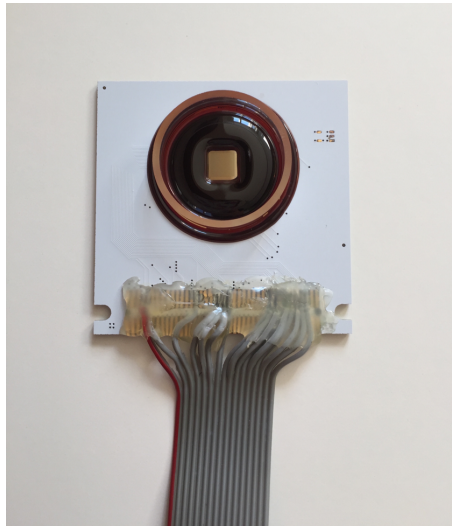


Figure 3.11: **Image of the 16-wires flat cable soldered to the 3Brain BioChip 4096E pads corresponding to the stimulation electrodes.** The connections are at the end covered by a layer of silicone to isolate them from the external environment and strengthen them against humidity, since the system must stay in incubation at 37°C.

Before starting the measures, it is recommended to execute a fixture compensation on the 4294A impedance analyzer, which is an operation aimed to preserve the measurement accuracy when the instrument is connected to the device through the test fixtures. In particular the *open/short* compensation is usually performed [38].

### 3.6 Arduino® Micro and CD4067 multiplexers

Each time an impedance measurement is conducted, a couple of the flat cable wires must be chosen and manually connected to the impedance analyzer leads. In this thesis project a platform has been joined to the measurement equipment in order to automate the electrodes choice without the user handling the flat cable. This is possible thanks to the integration of an Arduino® Micro and two CD4067B CMOS Analog multiplexers on a breadboard.

The Arduino® Micro technical specifications are reported in table 3.3.

Table 3.3: Arduino® Micro technical specifications. [41]

Microcontroller	ATmega32u4
Operating voltage	5V
Digital I/O pins	20
Analog Input Channels	12
PWM Channels	7
DC current per I/O pin	40mA
Flash memory	32 KB (ATmega32u4)
SRAM	2.5 KB (ATmega32u4)
EEPROM	1 KB (ATmega32u4)
Clock Speed	16 MHz

The CD4067B is a 16-channel multiplexer, i.e. it presents 16 input channels and one output. Its technical features are reported in table 3.4. The terminal assignment for this device and for Arduino® Micro are reported in figure 3.12.

Table 3.4: CD4067B multiplexer technical specifications. [42]

Configuration	16:1
Power supply type	Single or Dual
Vss (min)	-5V
Vss (max)	0V
Vdd (min)	3V
Vdd (max)	18V
ON resistance	125Ω
Operating temperature	-55 to 125°C
DC input current	10mA

The electrical scheme of the complete circuit, realized by the *KiCad* software, is reported in figure 3.13, while a picture of the circuit is reported in figure 3.14.

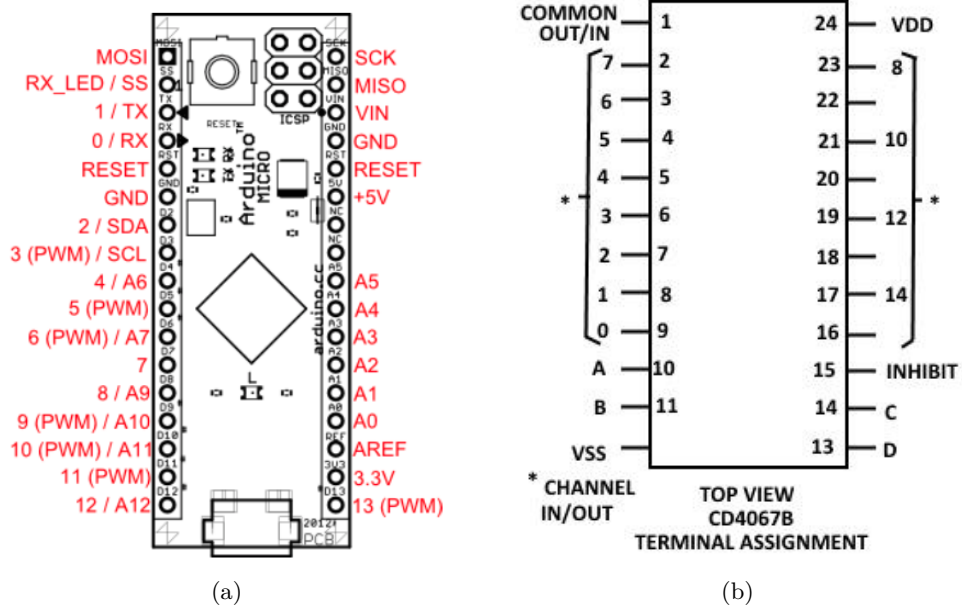


Figure 3.12: a) Terminal assignment for Arduino® Micro. [43]; b) Terminal assignment for CD4067B CMOS Analog multiplexer. [42]

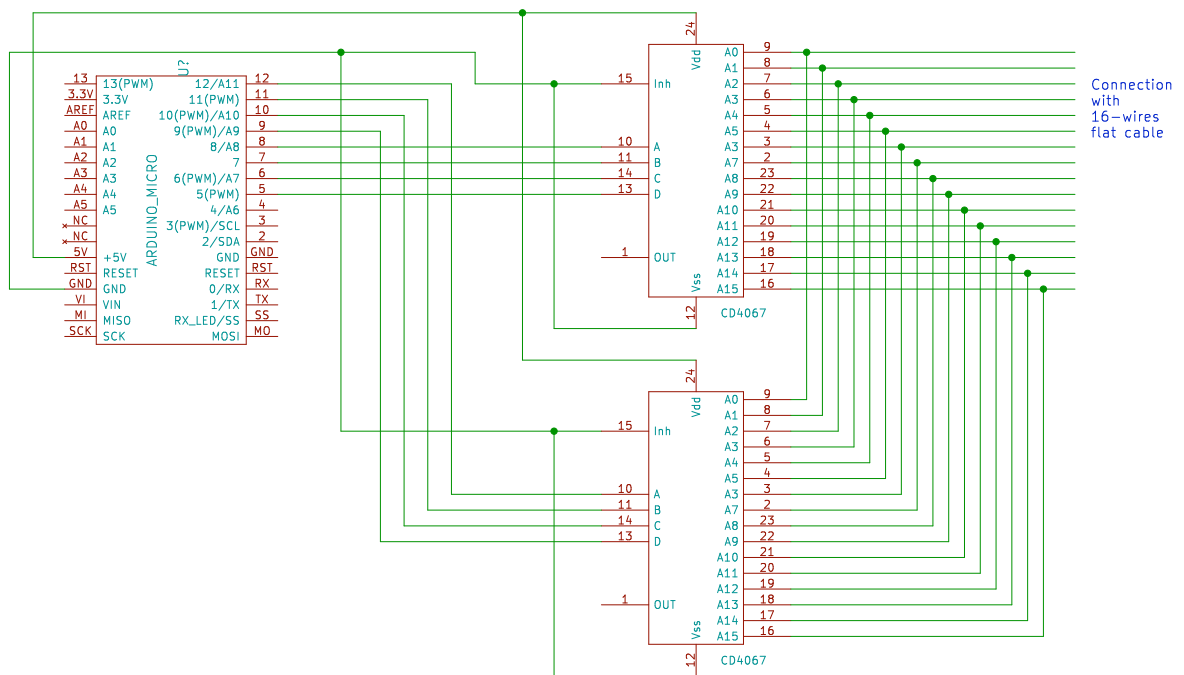


Figure 3.13: Electrical scheme of the circuit created.

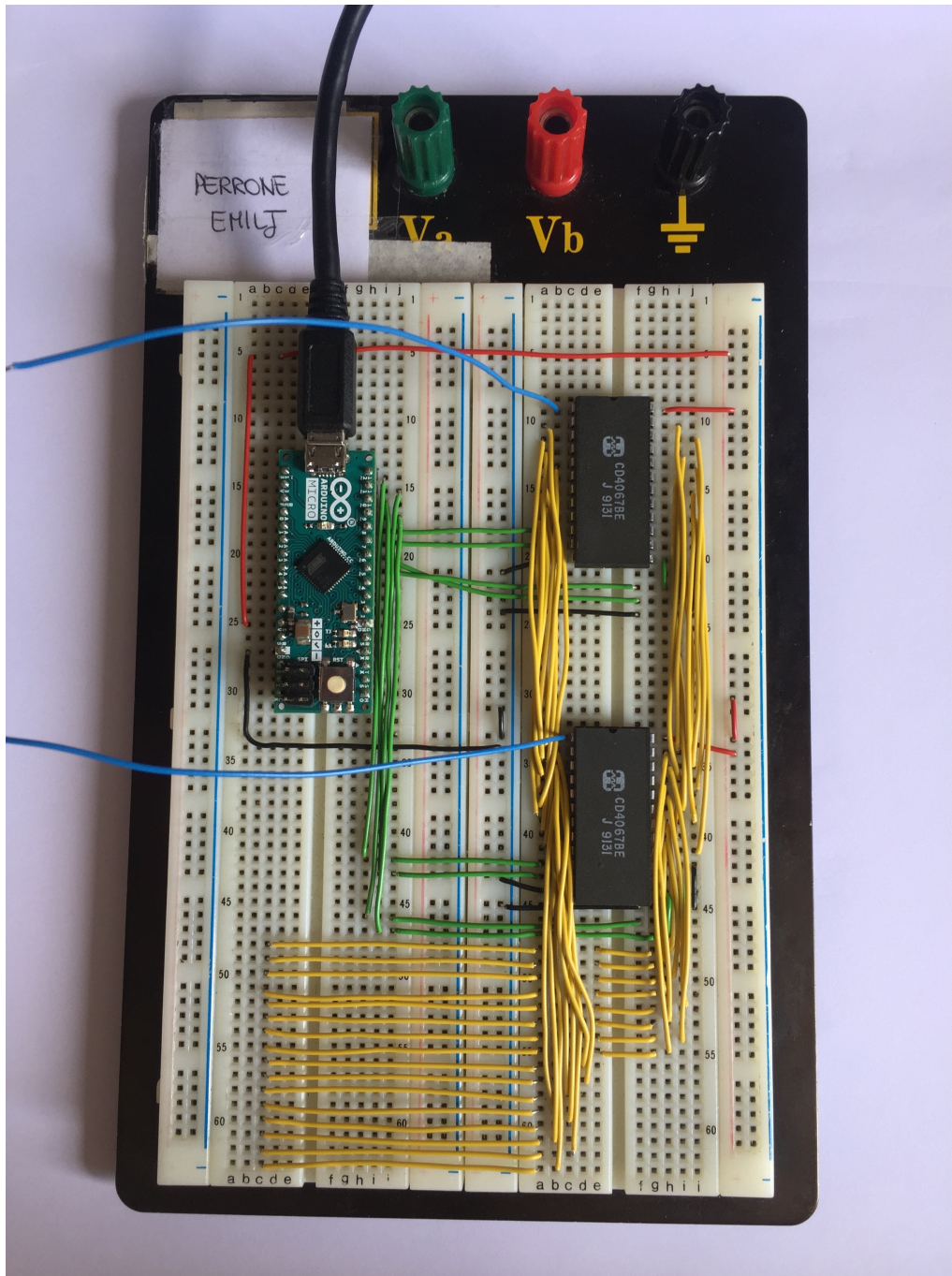


Figure 3.14: Electronic circuit created for choosing the electrodes for the impedance measurements.

It is not necessary to use an external power supply, because the Arduino® Micro is powered by the PC at 5V and it provides the power supply to the multiplexers through its "5V" and "GND" pins.

The red wires are referred to the power supply (5 V), the black ones indicate the ground (GND), the green wires connect the digital I/O pins of the Arduino® Micro to the digital control pins of the multiplexers. The yellow wires are connected to the 16 I/O channels of each multiplexer and at the other extremity they are connected to the 16-wires flat cable soldered to the BioChip. The blue wires connect the multiplexers outputs to the Kelvin

clip leads of the 4294A.

The wires of the flat cable are connected to the 16 inputs of both the multiplexers, while the outputs of the multiplexers are connected to the clip leads of the impedance analyzer. Since each multiplexer presents 16 switches (from 0 to 15), four binary control inputs are necessary to select one channel. For each multiplexer these inputs, called A, B, C, D are connected to four I/O pins of Arduino® Micro, through which the binary sequence for allowing the selection of one channel is sent. The CD4067B truth table is reported below (table 3.5). If the inhibit input is set to a logic "1", all the channels are off.

Table 3.5: CD4067B multiplexer truth table. [42]

A	B	C	D	Inh	Selected channel
X	X	X	X	1	None
0	0	0	0	0	0
1	0	0	0	0	1
0	1	0	0	0	2
1	1	0	0	0	3
0	0	1	0	0	4
1	0	1	0	0	5
0	1	1	0	0	6
1	1	1	0	0	7
0	0	0	1	0	8
1	0	0	1	0	9
0	1	0	1	0	10
1	1	0	1	0	11
0	0	1	1	0	12
1	0	1	1	0	13
0	1	1	1	0	14
1	1	1	1	0	15

Once the circuit is terminated, the Arduino can be connected to the PC through micro USB for loading the program created in the Arduino IDE for the selection of the measurement electrodes. A 4x4 LED matrix, reported in figure 3.15, was created on the front panel of a LabVIEW® interface referred to the settings. Each LED graphically corresponds to an electrode; these LEDs are indexed from 0 to 15. When the user clicks on two LEDs, a string is created, containing their indexes separated by a space and it is written on a serial port (the same connected to Arduino). For instance, if electrodes 3 and 11 are chosen, the string "3 11" is written.



Figure 3.15: LED matrix created in LabVIEW® to let the user choose the electrodes for conducting the impedance measurements directly from LabVIEW® graphical user interface.

In the Arduino integrated development environment (IDE), a program was implemented for reading the string from the serial port and sending through the output pins a specific binary sequence to the multiplexers, depending on the numbers contained in the string. This is made by executing a "switch case" instruction on the value of the numbers read from string. The values are converted and written on the output pins: the first value is written on the first group of 4 output pins and sent to the first multiplexer, while the second value is written on the second group of output pins and sent to the second multiplexer.

It is important to know that the indexes of the LED matrix are not the same as in the BioChip 4096E. As reported in figure 3.16, in the BioChip's datasheet the electrodes indexing starts from the lower left corner, while in the LED matrix in LabVIEW® it starts from the upper left corner. Hence, the table created in the Arduino program for the conversion keeps this difference into account. For example, if the user selects the LED '0', actually it corresponds to the electrode '12' on the BioChip, so the value '0' is converted into the binary sequence which codifies the value '12'.

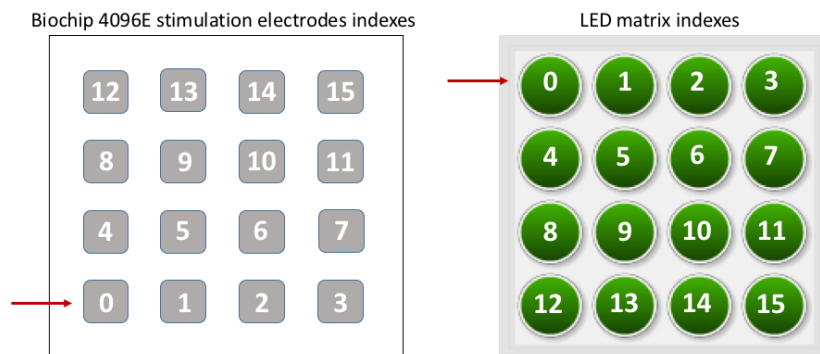


Figure 3.16: Comparison between the indexing of the real electrodes in the BioChip 4096E and of the LEDs in LabVIEW®. In the first case the indexing starts from the lower left corner, while in the second case it starts from the upper left corner.

The table developed for the conversion of the values contained in the string read from the serial port is reported in figure 3.17.

```
int muxChannel[16][4] = {
    {1,1,0,0}, //LED 0 (electrode 12)
    {1,1,0,1}, //LED 1 (electrode 13)
    {1,1,1,0}, //LED 2 (electrode 14)
    {1,1,1,1}, //LED 3 (electrode 15)
    {1,0,0,0}, //LED 4 (electrode 8)
    {1,0,0,1}, //LED 5 (electrode 9)
    {1,0,1,0}, //LED 6 (electrode 10)
    {1,0,1,1}, //LED 7 (electrode 11)
    {0,1,0,0}, //LED 8 (electrode 4)
    {0,1,0,1}, //LED 9 (electrode 5)
    {0,1,1,0}, //LED 10 (electrode 6)
    {0,1,1,1}, //LED 11 (electrode 7)
    {0,0,0,0}, //LED 12 (electrode 0)
    {0,0,0,1}, //LED 13 (electrode 1)
    {0,0,1,0}, //LED 14 (electrode 2)
    {0,0,1,1} //LED 15 (electrode 3)
};
```

Figure 3.17: Conversion table used in the Arduino program.

The following flowcharts report all the instructions executed by the Arduino program for the electrodes choice. The flowchart in figure 3.18 is the general flowchart for the entire program, while the flowcharts in figures 3.19 and 3.20 report the content of the blocks 1 and 2 for the switch case instructions executed for both the values read from the string on the serial port.

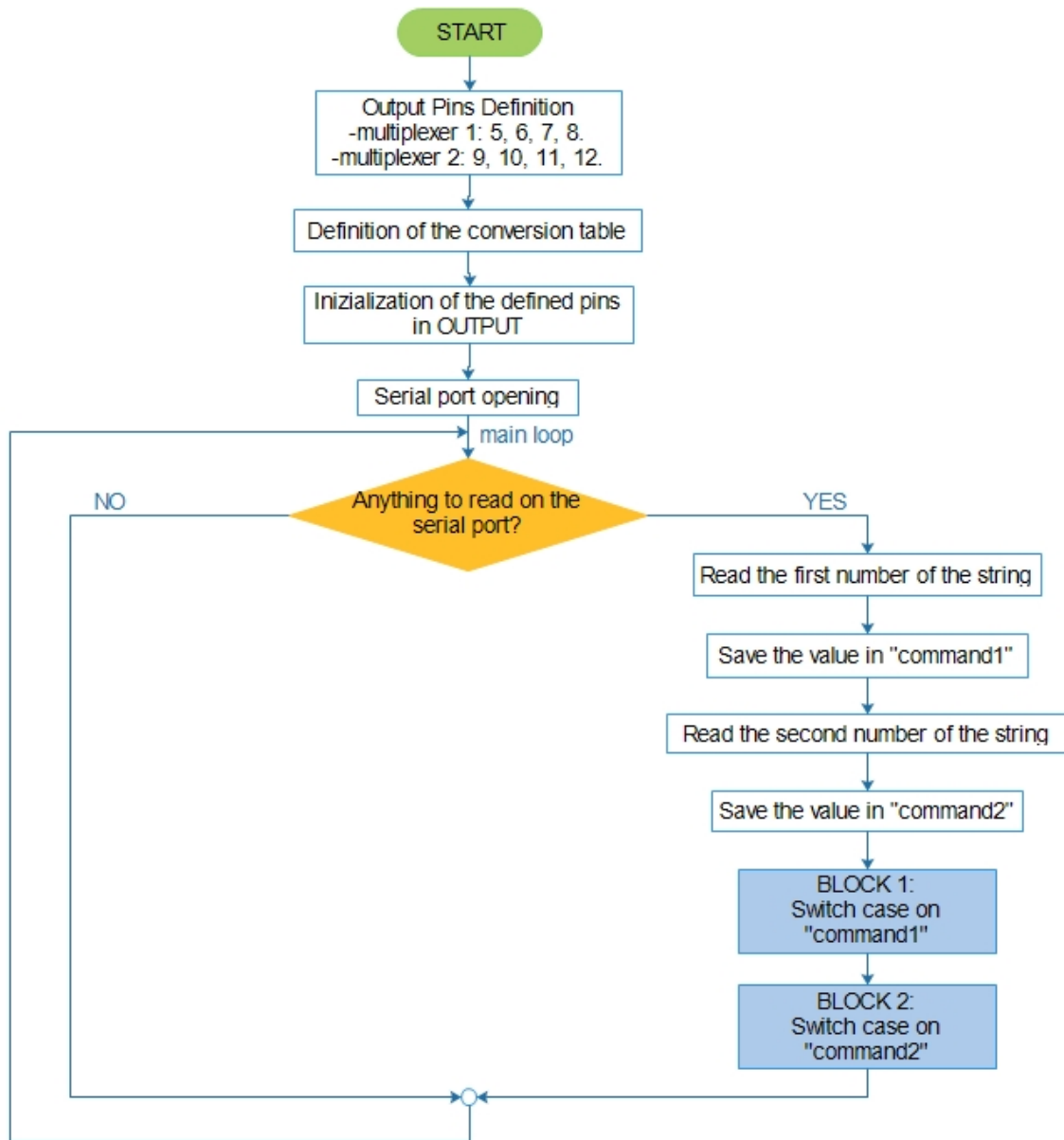


Figure 3.18: **General flowchart of the Arduino® program working principle.** BLOCK 1 and BLOCK 2 are explained in detail in the next flowcharts.



Figure 3.19: Flowchart of the "switch case" instruction executed for the conversion of the first number read from the string (BLOCK 1).



Figure 3.20: Flowchart of the "switch case" executed for the conversion of the second number read from the string (BLOCK 2).

## Chapter 4

# Impedance Measurements and data elaboration

### 4.1 Experiments timeline

As explained in the previous chapter, before starting the drug screening experiments, a series of trials must be executed for ensuring cells adhesion on the BioChip 4096E electrodes surface. With the purpose of evaluating cells adhesion, the following timeline was respected, reported also in figure 4.1:

1. BioChip's preconditioning procedure (48 hours, 37°C).
2. Impedance monitoring (48 hours) of the culture medium without cells.
3. Coating of the BioChip's active area with collagen type I (overnight, 4°C).
4. Cells seeding.
5. Impedance monitoring (48 hours) immediately after cells seeding.

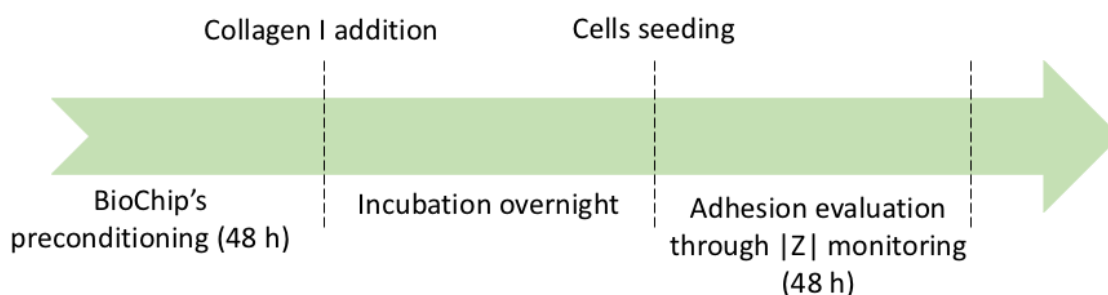


Figure 4.1: **Timeline followed for assessing cells adhesion on the BioChip 4096E.**

Once adhesion was established, Etoposide was added to the cell culture, with the following timeline, reported also in figure 4.2:

1. BioChip's preconditioning procedure (48 hours, 37°C).
2. Impedance monitoring (48 hours) of the culture medium without cells.
3. Coating of the BioChip's active area with collagen type I (overnight, 4°C).

4. Cells seeding.
5. Impedance monitoring immediately after cells seeding.
6. Addition of the drug to the cell culture in the exponential phase of its growth.
7. Impedance monitoring immediately after the addition of Etoposide.

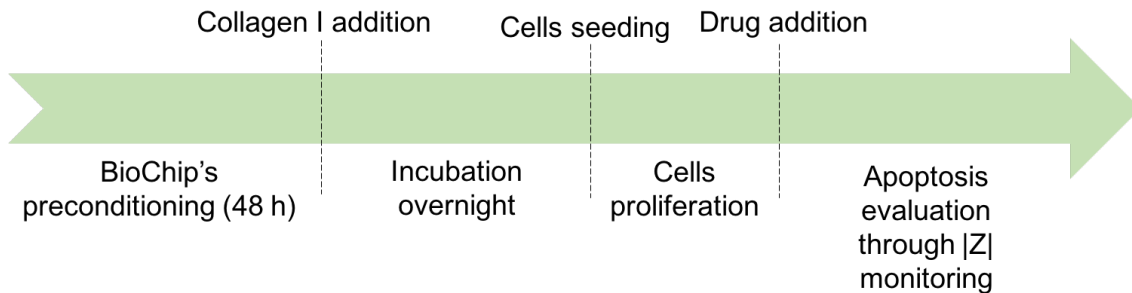


Figure 4.2: Timeline followed for evaluating the effect of the drug on the cell culture in the BioChip 4096E.

As mentioned before, impedance measurements through the ECIS technique are conducted executing a frequency sweep. This allows to choose the frequency value at which the system has the maximum response. Specifically, a sweep measurement was executed:

- at the end of the preconditioning phase, when the chip was filled uniquely with the culture medium, for having a background condition;
- after 24 hours from cells seeding on the chip.

The  $|Z|$ - $f$  curves obtained from these measurements were compared; the frequency at which the maximum difference between the curves occurred was chosen as the measurement frequency for the next analysis. After conducting the single measurement for establishing the correct measurement frequency, it was possible to use it for a monitoring measurement over time, in order to obtain the impedance evolution associated to the cells status [13] [25]. In the case of proliferation monitoring, impedance should increase [14], while after the administration of the drug to the cell culture, a decrease in impedance modulus would be expected during time [12].

## 4.2 LabVIEW® Graphical User Interface

In order to obtain a friendly user interface for the utilisation of the impedance analyzer, the LabVIEW® (*National Instruments Corp.*) IDE was employed and a program was implemented to command the instrument. This was feasible thanks to the presence of a specific driver for interfacing the 4294A with LabVIEW®, capable of replicating all the operations which can be set through the impedance analyzer keyboard. Downloading this driver, it is possible to have access to a series of VIs (virtual instruments) specific for 4294A, each of which has a precise function. For connecting the impedance analyzer with the LabVIEW® program on the PC, a GPIB (General Purpose Interface Bus) IEEE 488.2 from *National Instruments* was used.

The LabVIEW® Graphical User Interface created consists of a tab control, which is a panel including more pages. In the present GUI, the tab includes 3 pages: "*settings*",

"single measurement" and "monitoring over time".

The flowchart in figure 4.3 reports the logical steps executed for conducting the impedance measurements.

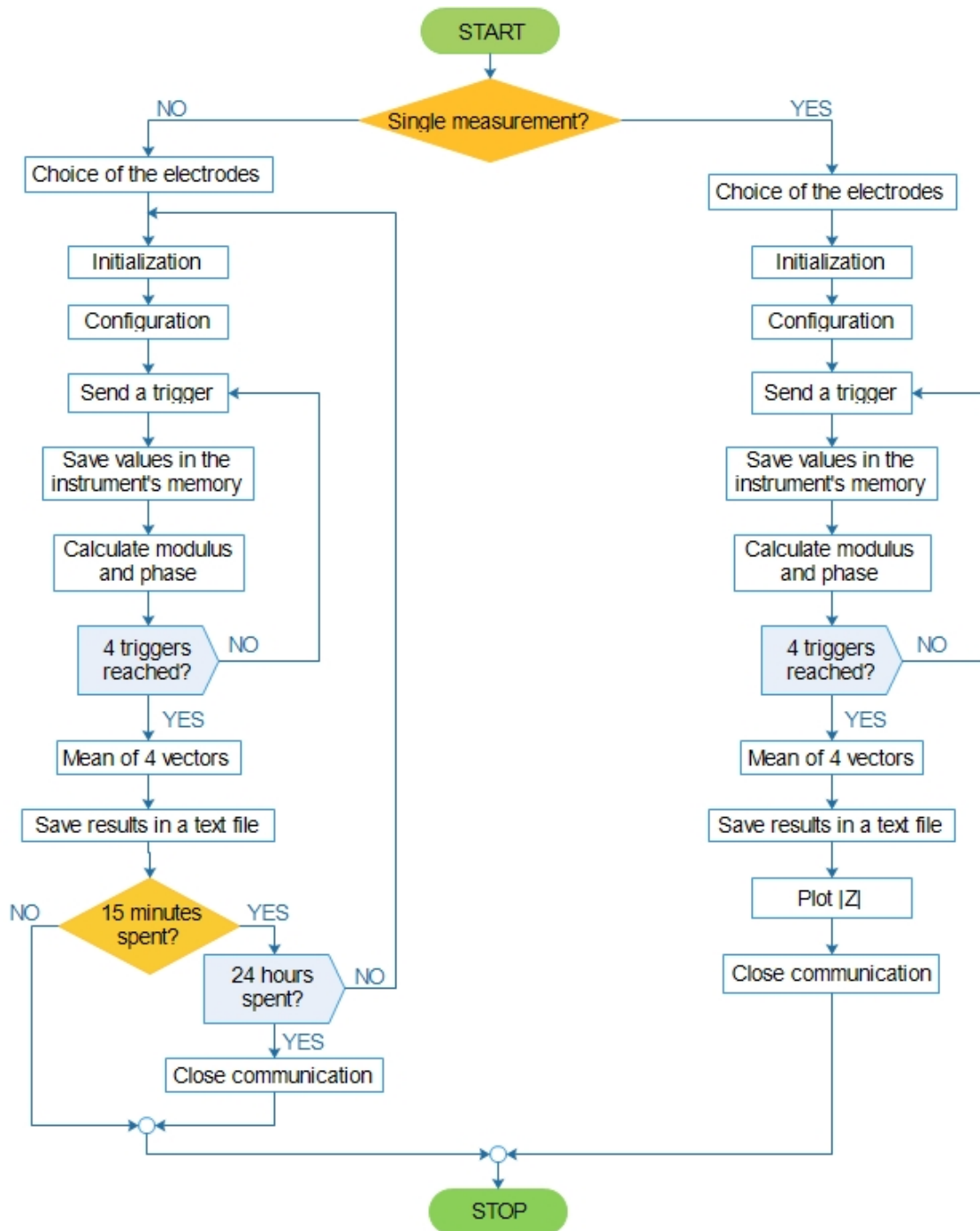


Figure 4.3: General flowchart explaining the operations executed by the LabVIEW® program for the impedance measurements.

### 4.2.1 Settings configuration

The first page ("settings") contains all the controls for choosing the measurement settings. The controls on the right side are related to the single measurement settings, to the monitoring settings or to both. The controls "sweep.start" and "sweep.stop", useful for the single measurements, are for the frequency sweep start and stop values; the control "NPoints" is useful for choosing the number of points constituting the impedance curve for each measurement. The "VISA" control is for choosing the address of the device to be initialized for establishing a communication, in this case a GPIB communication. The "COM" control is instead for choosing the serial port to which the selected indexes of the LED matrix will be sent to the Arduino® Micro.

The controls "monitoring.center" and "monitoring.span" are for the insertion of the chosen frequency (at the end of the single measurements) for the monitoring phase; through the control "wait" the user can establish how many seconds to wait for executing the next measurement. In this case, it is generally set to 900 or 1800 seconds (15 or 30 minutes). The control "Tmeasure" is for choosing the duration of the monitoring measurements, for instance 24 hours.

The control "oscLevel" allows to insert the value of the test voltage for the measures. The LED matrix, as explained before, allows the user to choose the couple of electrodes for conducting the impedance measurements. Once the electrodes are selected, clicking the button "apply", the next two pages, related to the measurements are enabled.

Figure 4.4 shows how the page is structured.

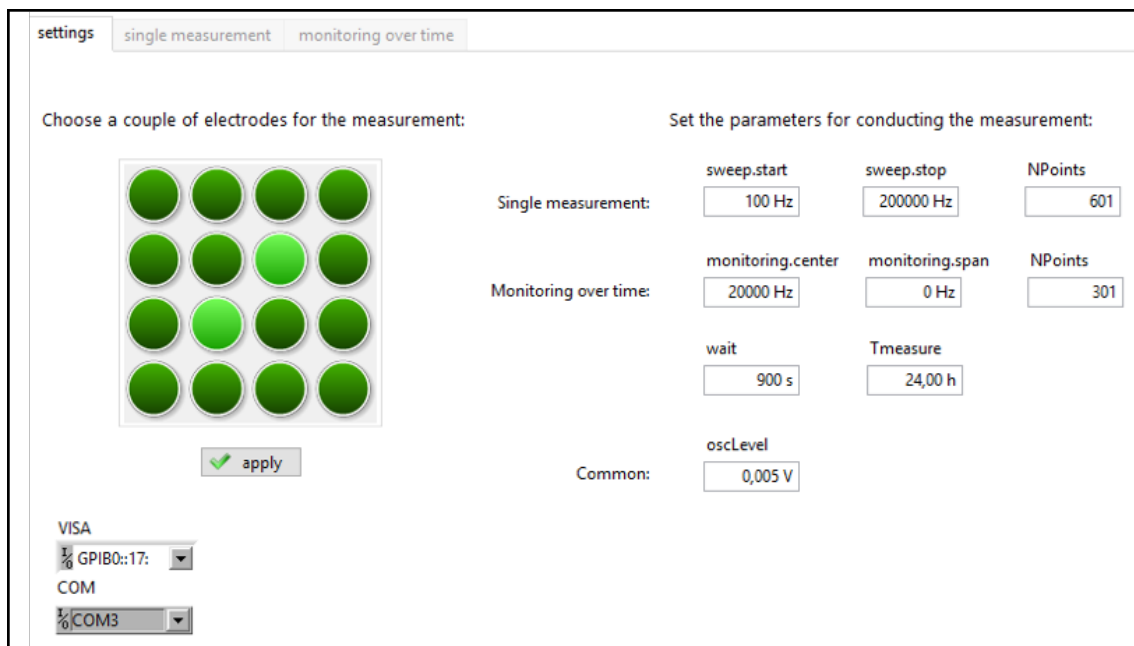


Figure 4.4: "Settings" page of the tab control in the LabVIEW® GUI.

With regard to the single measurements, in literature many different frequency ranges have been tested, for instance 1 kHz - 1 MHz [12], 100 Hz - 100 kHz [44], 500 Hz - 64 kHz [23], etc.; however, they are generally included in the range 1 Hz - 100 MHz. In this case, the range 100 Hz - 200 kHz was chosen and tested. Even for the test voltage signal, many values can be found, ranging from 10  $\mu V$  to 1 V [13][25][45]. In this project, four different voltages were tested (5, 10, 50, 100 mV), in order to choose the most appropriate value.

## 4.2.2 Single measurement

The single measurement is performed before starting an impedance monitoring over time in order to choose the frequency at which the impedances of the system with and without cells have the maximum difference and employ it for the successive measures [13]. Since the modality for sending triggers to the instrument is common for single measurement and monitoring over time, a subVI was created and used for both the options, called *subVI\_sendTrigger*. The triggers are sent from the software to the instrument through GPIB connection. With regard to the configuration parameters, not all of them are common to the single measurement and the monitoring modes; hence another subVI was created (*subVI\_configuration*) for the common settings, while the different settings can be inserted manually through the user interface controls. All the settings of *subVI\_configuration* in single measurement mode are reported in table 4.1.

Table 4.1: Resuming table of all the commands set in 4294A for configuring the device to ECIS measurements (single measurements).

Parameter	Configuration
Configure adapter	NONE
Configure measurement	$ Z -\theta$
Configure sweep	Frequency
Direction	UP
Sweep type	Logarithmic
Number of points (NPoints)	601
Configure oscillator	Voltage
Voltage level	5 mV ÷ 100 mV
Configure sweep range	Start (100 Hz)/Stop (200 kHz)
Bandwidth	2
Display split	YES (Trace A: $ Z $ , Trace B: $\theta$ )
Y axis scale	Linear
Trigger mode	Number of groups (4)
Trigger source	bus (GPIB)

As can be seen from the table, different voltage test signal levels were used to conduct the measure. In particular 5 mV, 10 mV, 50 mV and 100 mV signals were tested for evaluating cells response and choose not only the correct frequency but also a test signal adequate enough to obtain a smooth  $|Z|$  curve without electrically stressing cells [25]. Figure 4.5 reports the block diagram of the *subVI\_configuration* for the single measurement mode.

In the *subVI\_sendTrigger*, there are the blocks used to send a trigger to the instrument for starting a sweep, measure and save the measured values. Since one sweep measure corresponds to one trigger, for increasing the stability of the measures, it was chosen to execute a certain number of triggers and then implement an averaging operation. In this specific case, four triggers are sent, according to the trigger mode set in *subVI\_configuration* (number of groups = 4). Once the triggers are executed, four arrays are obtained and the measured values are expressed in terms of real and imaginary part, hence a conversion into modulus and phase is required. After the conversion, *subVI\_sendTrigger* terminates and the average is executed between these four vectors; this is done both for modulus vectors and phase vectors. At the end two vectors of NPoints columns are obtained, one for mod-

ulus and one for phase. Since the first is most significant for impedance measurements, the modulus vector is plotted on a  $XY$  graph on the user interface as a function of the frequency sweep, in order to replicate the curve on the 4294A display. The block diagram of *subVI\_sendTrigger* is shown in figure 4.6 and is common for the single measurement and monitoring modes.

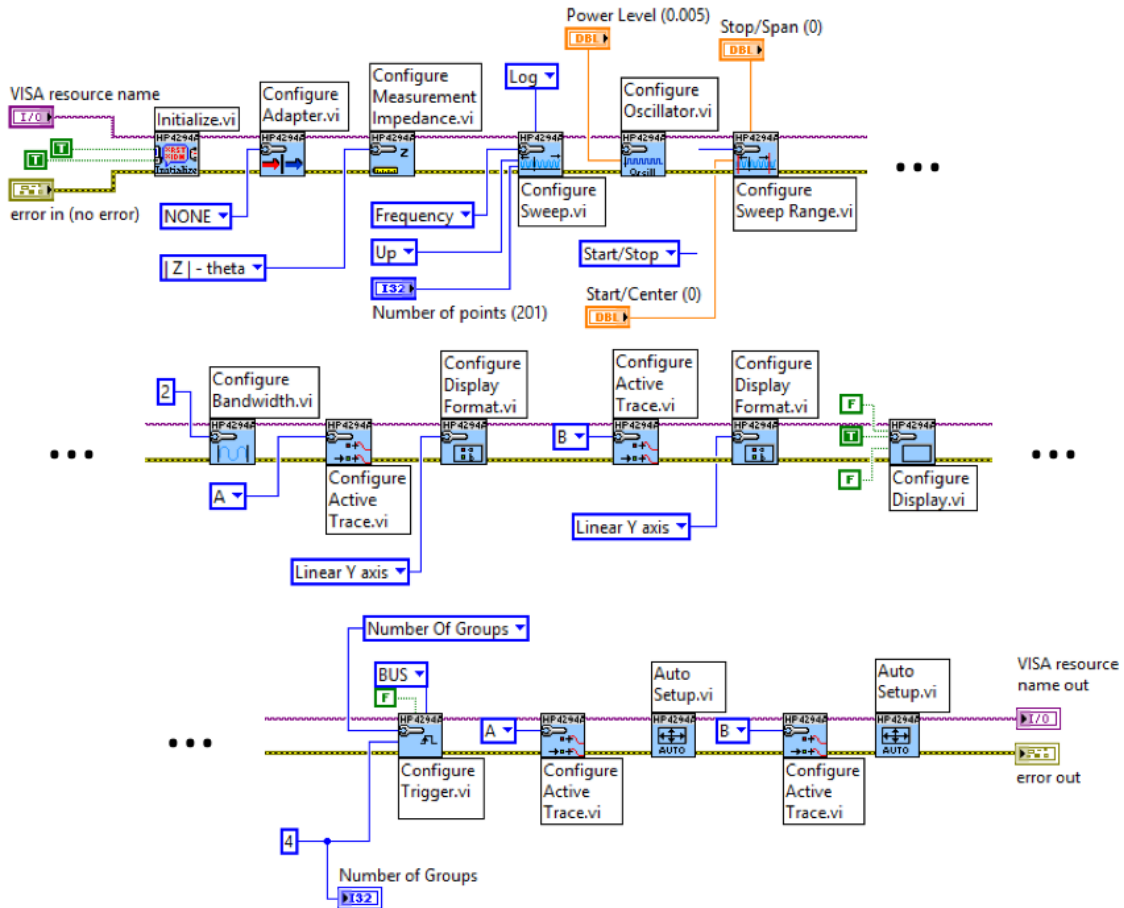


Figure 4.5: Content of the *subVI\_configuration* for impedance single measurement.

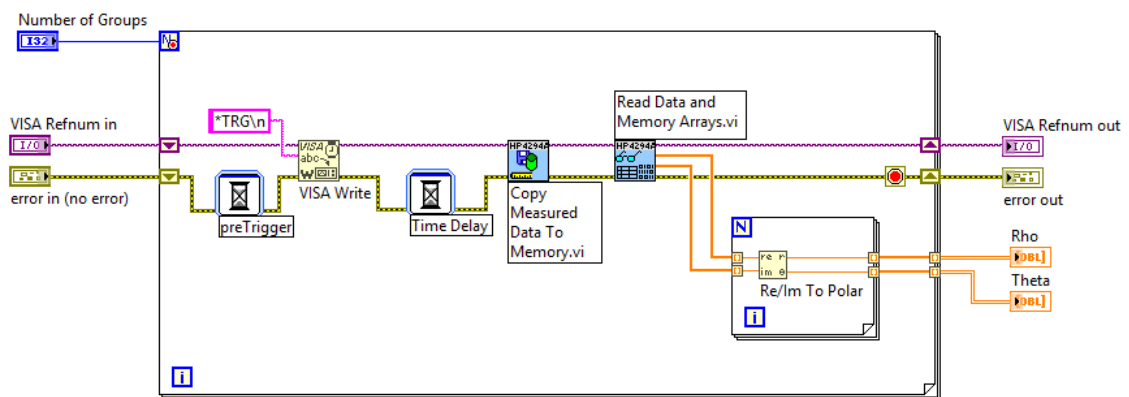


Figure 4.6: Content of the *subVI\_sendTrigger*.

Data are saved in a text document, in form of 3 column vectors, i.e. modulus, phase and frequency sweep of length NPoints. An example is shown in figure 4.7.

Mean  Z	Mean theta	Sweep
1287430.09	-1.04	100
1277661.67	-1.02	102
1212776.86	-1.03	103
1275610.4	-1.07	105
1277333.61	-1.07	106
1314072.04	-1.03	108
1199062.34	-0.98	110
1279631.14	-0.99	111
1191043.12	-1.06	113
1236921.07	-0.98	115
1252700.37	-1.05	117
1086918.73	-1.02	118
1149324.11	-1.06	120
1132164.68	-1.07	122
1098611.43	-1.01	124
1119187.08	-1.08	126
1082440.01	-1.05	128

Figure 4.7: Extract of the structure of the text document created after each measurement.

Figure 4.8 shows the "Single measurement" page of the control tab in the LabVIEW® GUI.

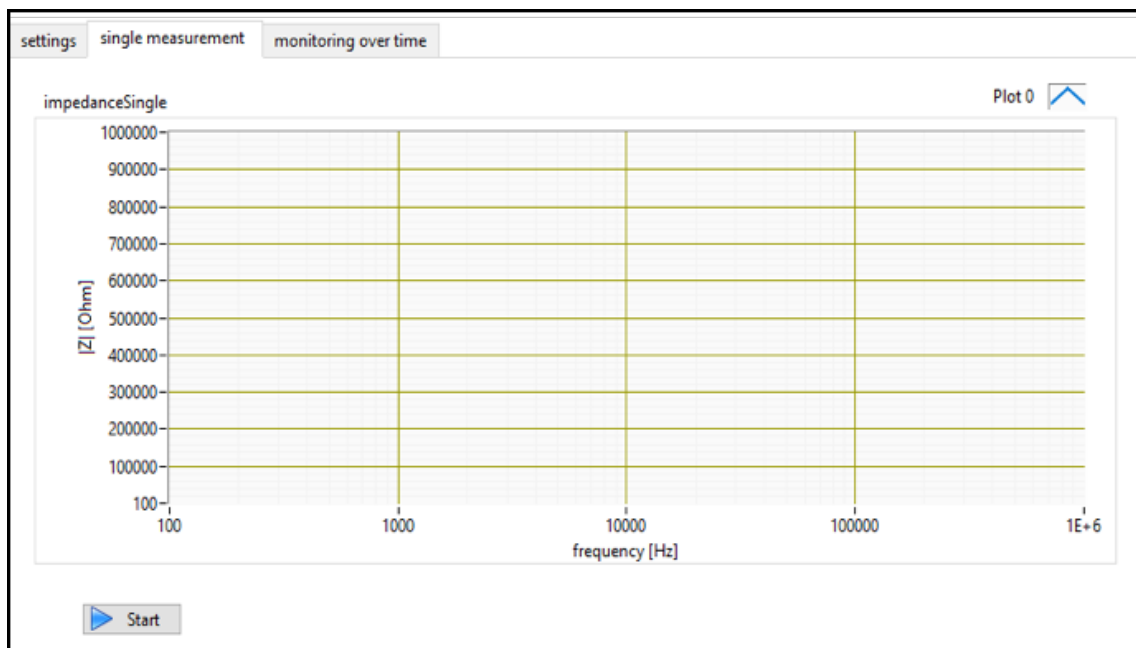


Figure 4.8: "Single measurement" page of the tab control in the LabVIEW® GUI.

When the "Start" button is pushed, the single measure starts and is executed as mentioned before. At the end of the measurement, the impedance modulus is plotted on the graph in function of the frequency.

Once the measures are conducted, the data obtained from LabVIEW® are loaded and elaborated in Matlab® R2018a. A Matlab script was created to read the data from a text document and save them into a  $NPoints \times 3$  matrix. To select the correct stimulation frequency, the modulus vector is plotted in function of the frequency sweep points in a modulus-frequency log-log graph [11]. By overlapping the curves related to the measures on the chip in presence of fresh medium and in presence of cells, it is possible to identify the stimulation frequency, i.e. the frequency at which the difference between the curves is maximum. Figure 4.9 reports a theoretical representation of the graph which should be obtained [25].

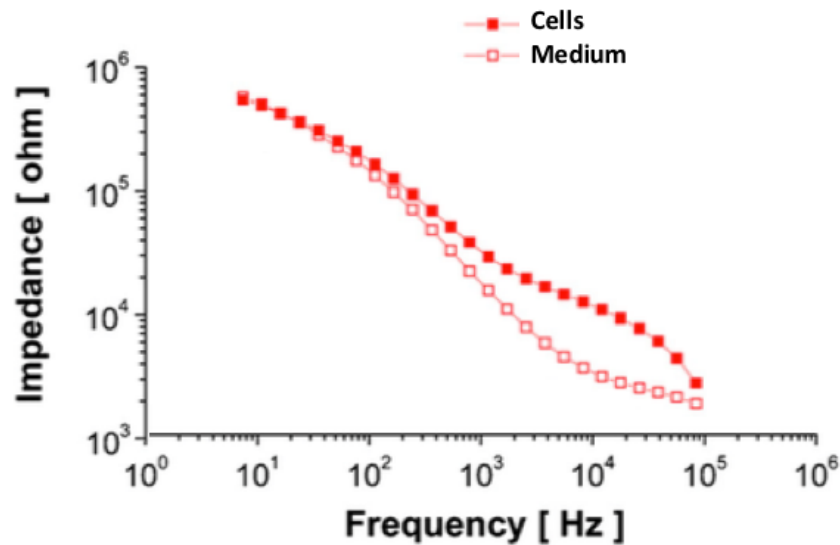


Figure 4.9: Theoretical trend of the overlapped impedance curves when the chip’s chamber is filled with medium or seeded with cells. After plotting this graph, the frequency at which the maximum difference between the curves is found, is chosen as the stimulation frequency for the subsequent monitoring phase. [25]

### 4.2.3 Impedance monitoring over time

Once the stimulation frequency is established, it could be interesting to conduct a prolonged impedance measurement in order to have a real-time control of cells activity. In fact through the impedance monitoring over time, it is possible to assess cell adhesion, proliferation, confluence and detachment from electrodes, due to cell death. Hence, in the present work, the impedance monitoring was used both for establishing cells proliferation and for evaluating the effects of Etoposide on the cell culture on the BioChip. In the developed LabVIEW® program impedance measures are executed in the same way of single measurements but cyclically, every 15 or 30 minutes. All the settings of *subVI\_configuration* in the monitoring mode are reported in table 4.2 and the *subVI\_configuration* block diagram is shown in figure 4.10.

All the operations for sending the triggers are equal to the single measurement mode, hence the block diagram is not reported again and is shown in figure 4.6, page 64.

In this case, since a precise frequency value for cell stimulation is desired, the options "Center-Span" are set for the sweep range configuration in the "Settings" page, by selecting the chosen frequency as the center frequency and 0 Hz as the span. Nevertheless, the span is never precisely 0 Hz, but a very little range (i.e. 20 Hz) around the center value. This

Table 4.2: Resuming table of all the commands set in 4294A for configuring the device to ECIS measurements (impedance monitoring over time).

<b>Parameter</b>	<b>Configuration</b>
Configure adapter	NONE
Configure measurement	$ Z -\theta$
Configure sweep	Frequency
Direction	UP
Sweep type	Logarithmic
Number of points (N_points)	301
Configure oscillator	Voltage
Voltage level	50 mV
Configure sweep range	Center (20 kHz)/Span (0 Hz)
Bandwidth	2
Display split	YES (Trace A: $ Z $ , Trace B: $\theta$ )
Y axis scale	Linear
Trigger mode	Number of groups (4)
Trigger source	bus (GPIB)

is not relevant for the measurement, because a mean of the NPoints of each measurement is plotted over time.

As for single measurements, in the monitoring mode data are saved in a text document. This text file is updated after each measurement: when a measure is completed data are added to the data already saved.

The "Monitoring over time" page of the GUI contains a "Start" button, for starting the monitoring, which continues until 24 hours have elapsed or until the user pushes the "Stop" button. The indicator "NMeas" is an index which increments each time a measurement is finished. In the indicators "First measure" and "Last measure" the indications about the time of the first measure and the current one are reported. The first timer increments every second and is reset to zero each time a new measure starts. The second timer increments every second from the first measure on. The "operation" indicator gives information about the measure's status: the messages "measuring..." or "measure finished" might be displayed. Figure 4.11 shows the "Monitoring over time" page of the control tab in the LabVIEW® GUI.

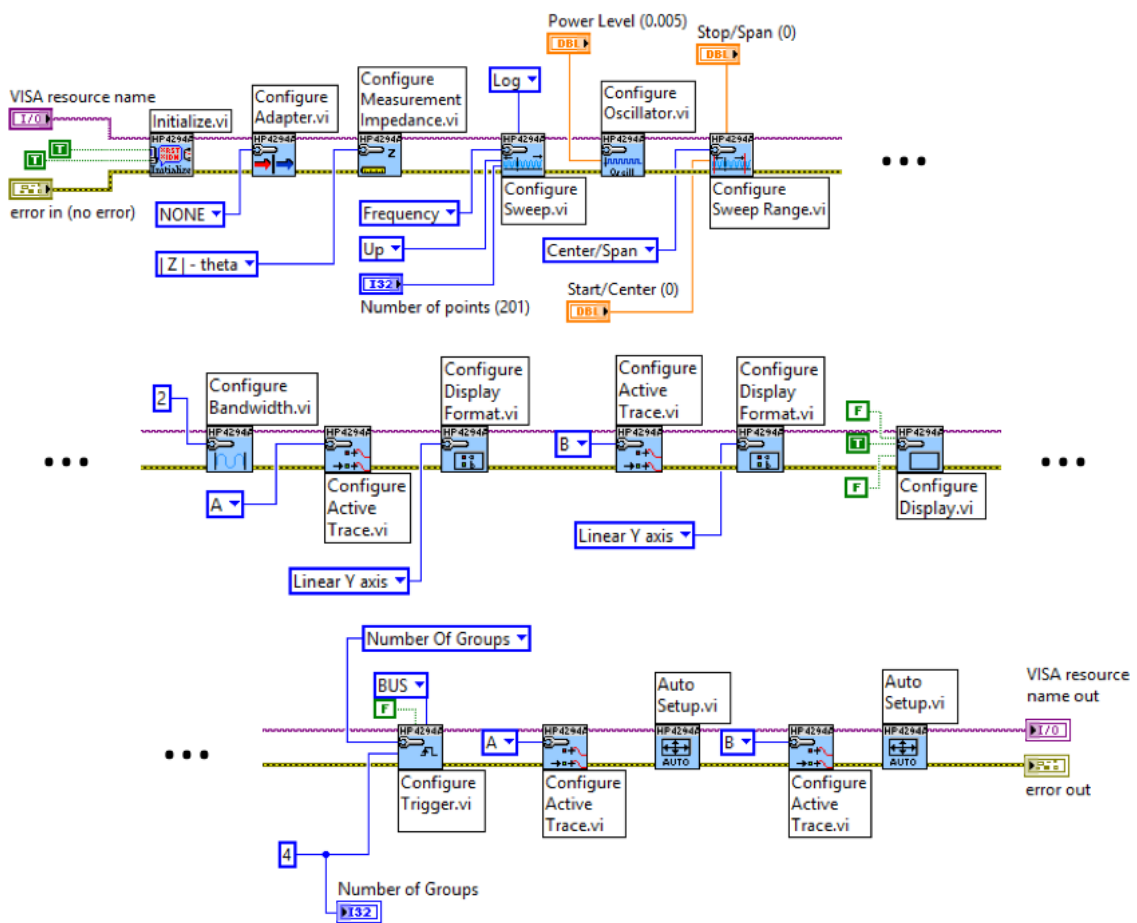


Figure 4.10: Content of the *subVI\_configuration* for impedance monitoring over time.

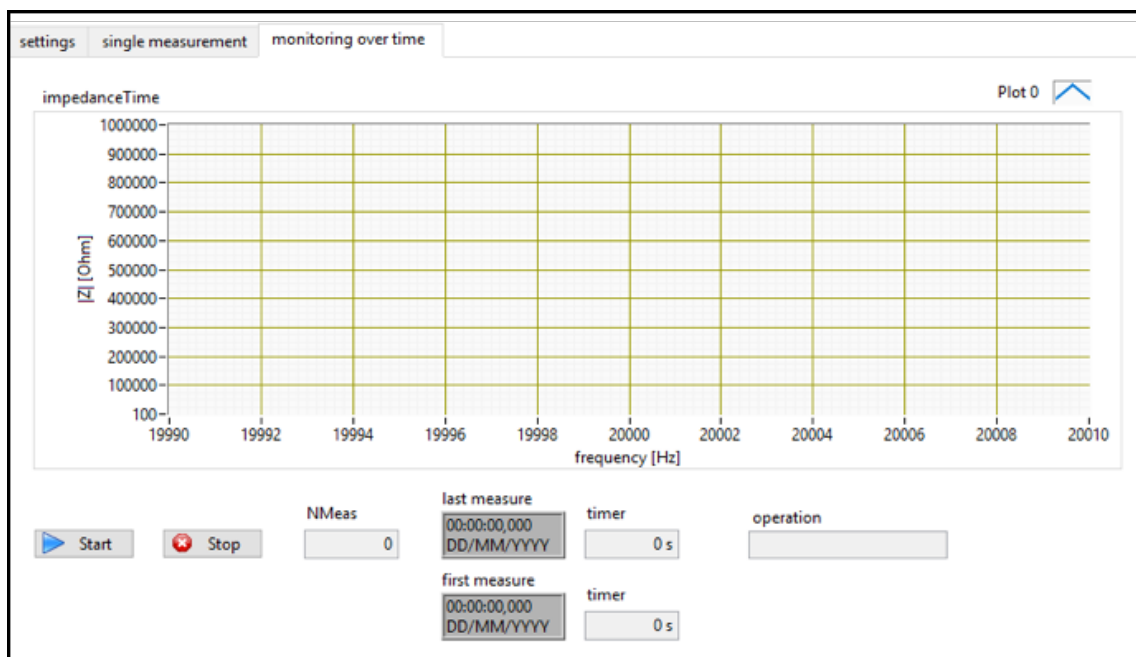


Figure 4.11: "Monitoring over time" page of the tab control in the LabVIEW® GUI.

Even in this case data are loaded in Matlab® and saved in a  $(NPoints \cdot NMeas) \times 2$  matrix. The third column is deleted because it is referred to the sweep, not relevant in the monitoring phase. For understanding cell behaviour, it is interesting to plot the impedance modulus in function of time, in order to assess their activity for example during 24 or 48 hours. Figure 4.12 shows a theoretical trend of the impedance modulus over time [14].

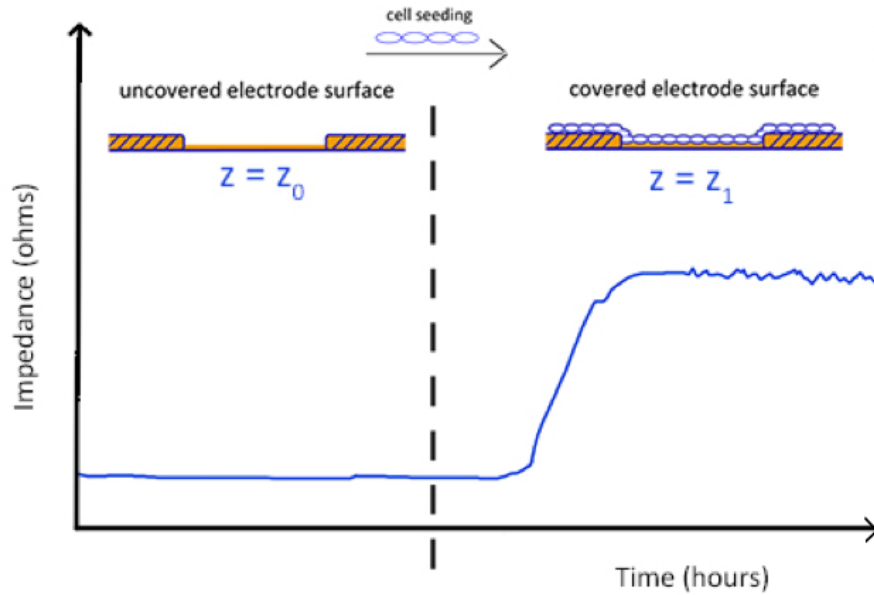


Figure 4.12: **Theoretical trend of impedance modulus in the case of monitoring over time.** The value  $Z_0$  represents measured impedance on the chip without cells; the value  $Z_1$  is the measured impedance in presence of cells adhered on the electrodes surface. As can be seen,  $Z_1 > Z_0$ . [14]

Sometimes normalized values are used to represent the impedance evolution during time, such as an index which plots the impedance trend in relation to the impedance measured at time 0. This index is an adimensional parameter and it is calculated as follows [46]:

$$\frac{|Z_c(i)|}{|Z_c(0)|} \quad (4.1)$$

where  $|Z_c(i)|$  is the impedance modulus at time point  $i$  in presence of cells and  $|Z_c(0)|$  is the impedance modulus in presence of cells but at time point 0.



## Chapter 5

# Results and discussion

This chapter reports the results obtained respectively with regard to the cellular adhesion assessment and to the evaluation of the drug's effect conducted over the BioChip 4096E seeded with HT-29 cells. A validation analysis is also reported for each test executed, to demonstrate the reliability of the proposed method in drug screening research.

### 5.1 Evaluation of the cellular adhesion and proliferation

Different combinations of parameters were used in order to optimize the culture protocol of HT-29 cells on the BioChip 4096E. The number of cells to be seeded and the collagen quantity for the coating treatment were varied several times with the aim of increasing the adhesion degree on the electrodes area. Some of the tests carried out, together with the issues encountered, are listed in table 5.1.

Table 5.1: Table reporting all the combinations tested for improving cellular adhesion on the BioChip's surface.

Test executed	Result
Collagen 5 $\mu g/mL$ ; 2000 cells seeded	No differences visible between the case "medium without cells" and the case "medium with cells".
Collagen 5 $\mu g/mL$ ; 90000 cells seeded	Poor adhesion, due to the presence of a too high number of cells: they easily detach because of the reduced space.
Collagen 10 $\mu g/mL$ ; 50000 cells seeded	Better adhesion, but not yet acceptable.
Collagen 10 $\mu g/mL$ ; 50000 cells seeded; laminin 10 $\mu g/mL$	Good adhesion.

The best results in terms of cells adhesion were given by the combination of collagen 10  $\mu g/mL$ , 50000 cells seeded and laminin 10  $\mu g/mL$  added to the cells suspension before seeding: the results obtained from the impedance single measurements are reported in figure 5.1.

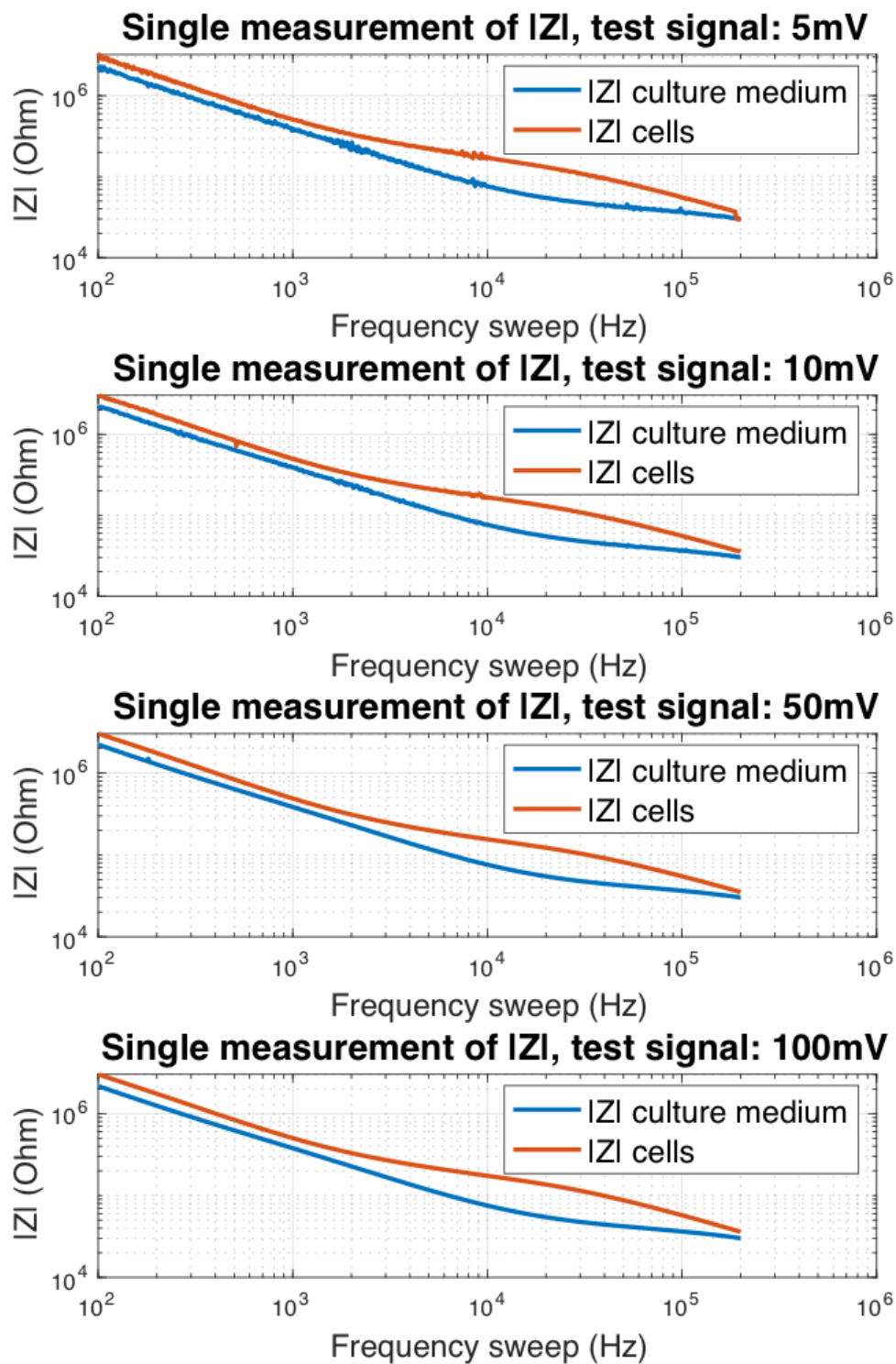


Figure 5.1: Matlab® plots of the overlapped curves referred to impedance measured with and without cells for assessing cells adhesion. The frequency sweep was executed from 100 Hz to 200 kHz and different voltage values were tested (5, 10, 50, 100 mV).

The graphs report the comparison between the impedance curve obtained in absence of cells and the curve obtained in presence of cells. The curves shape is similar to theoretical trend reported in figure 4.9 on page 66. Each graph is referred to a different voltage value. A good voltage value which allows to obtain smooth curves and is not so high to stress cells electrically is the voltage 50 mV. As mentioned before, the frequency sweep was made from 100 Hz to 200 kHz; as can be seen from the figure, the frequency at which the difference between the impedance curves is maximum is 20 kHz, hence it was chosen as the measurement frequency for the successive monitorings.

Once the single measurements were completed and the frequency and voltage value were chosen, the impedance monitoring over time was conducted to assess cell proliferation. The impedance curve referred to proliferation should have a trend similar to the cellular growth curve (figure 3.5, page 42), i.e. it should be possible to distinguish the lag phase, the log phase and the stationary phase.

Figure 5.2 reports the impedance evolution over time. A 120 hours monitoring was conducted; the first phase (a) is referred to the BioChip's preconditioning, in presence of only the culture medium. After this phase, a slow impedance growth (b) is visible, due to the presence of cells which start adhering. The slow growth phase is followed by the exponential phase (c), in which cells proliferate. The last phase of the curve is referred to the stationary phase (d), reached when all the available space on the electrodes area is filled. The results obtained are also in this case in accordance with the theoretical trend shown in figure 4.12 on page 69.

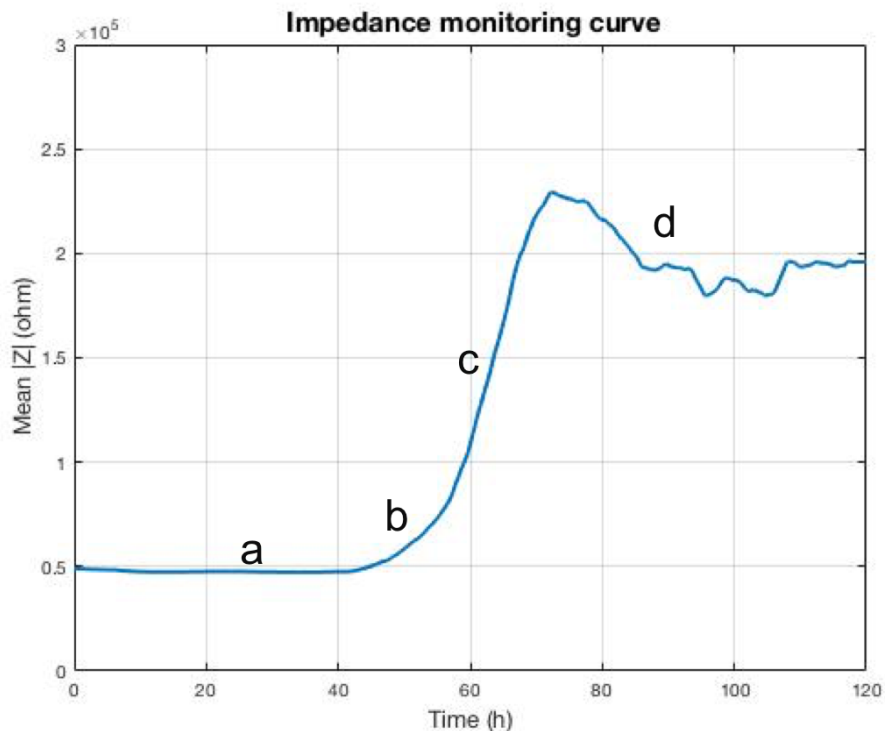


Figure 5.2: Matlab® plot of the impedance monitoring curve for assessing cells proliferation. The measures were executed every 15 minutes for 120 hours.

### 5.1.1 Validation assay

To assess cellular adhesion on the BioChip's electrodes area, a fluorescence microscopy analysis was conducted, through the Eclipse 80i (*Nikon*) microscope. A 20X immersion objective was employed, since the opacity of the BioChip's surface impedes to the light to cross it. For conducting the microscopy analysis, it was necessary to label cells: to this aim, the Vybrant® CFDA SE Cell Tracer Kit (V12883, *Invitrogen*) was used. The kit contains 10 vials of CFDA SE dye (500  $\mu\text{g}$  per vial) and one vial of DMSO and is kept at  $-20^\circ\text{C}$  before use.

CFDA SE (Carboxyfluorescein diacetate succinimidyl ester) is a dye that penetrates into the cell by diffusion and initially it is not fluorescent. The fluorescence is created when it enters the cell and is cleaved by esterases; subsequently it is able to form covalent conjugates with intracellular proteins, hence fluorescence is maintained within the cell. If the cell divides, the fluorescence is divided between the daughter cells and so on. By tuning the concentration of dye, it is possible to execute short (from 0,5  $\mu\text{M}$  to 5  $\mu\text{M}$ ) or long (from 5  $\mu\text{M}$  to 10  $\mu\text{M}$ ) experiments [47]. In this case, a short term experiment was necessary, hence a low concentration was chosen: 0,5  $\mu\text{M}$ .

The staining procedure was executed 24 hours after cell seeding and the protocol followed is described below [47]:

1. A reagents prewarming phase is necessary: 4 mL of PBS and 1,5 mL of fresh culture medium are prewarmed for 15 minutes at  $37^\circ\text{C}$ ; one vial of CFDA SE and the vial of DMSO from the kit are thawed out and kept at room temperature for 15 minutes. The following steps are conducted under laminar flow.
2. 90  $\mu\text{L}$  of DMSO are poured into a CFDA SE vial, obtaining a 10 mM solution.
3. 2  $\mu\text{L}$  of the solution created are diluted into 4 mL of prewarmed PBS, in order to obtain a concentration of 0,5  $\mu\text{M}$ .
4. The culture medium is aspirated from the cell culture on the BioChip and 1,5 mL of the diluted solution obtained at point 3 are poured into the chip's chamber. The system is kept in incubator ( $37^\circ\text{C}$ ) for 15 minutes.
5. The solution is aspirated and replaced by the prewarmed culture medium. The system is kept in incubator ( $37^\circ\text{C}$ ) for 30 minutes.
6. The BioChip is ready for microscopy analysis.

Figure 5.3 reports the results obtained from fluorescence microscopy. In particular, the results related to two different tests are reported:

- a. 90000 cells, collagen 5  $\mu\text{g}/\text{mL}$ ;
- b. 50000 cells, laminin 10  $\mu\text{g}/\text{mL}$ , collagen 10  $\mu\text{g}/\text{mL}$ .

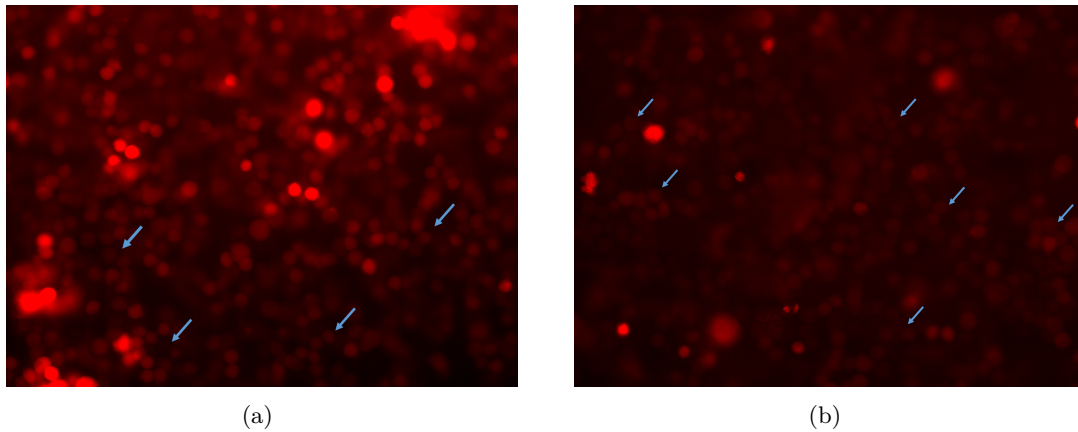


Figure 5.3: **Eclipse 80i (Nikon) fluorescence microscopy images (20X) for evaluating cellular adhesion on the BioChip's surface.** The results of two tests are reported: a) 90000 cells, collagen 5  $\mu\text{g/mL}$ ; b) 50000 cells, laminin 10  $\mu\text{g/mL}$ , collagen 10  $\mu\text{g/mL}$ .

As expected, the difference in the number of cells is well visible. In both cases there is a certain number of cells whose contours are vivid (blue arrows): these are spreaded cells. However there is also a number of cells that appear blurry: these are detached cells, because they are at a different depth. In figure 5.3(a) a greater number of blurry cells is visible in comparison to figure 5.3(b); this indicates that cells adhere better in the second case, when the collagen concentration is increased and laminin is added. Moreover, in case "a" a little shake of the BioChip on the stage of the microscope was enough to see cells moving, demonstrating the weakness of the cellular adhesion.

## 5.2 Evaluation of the effect of Etoposide

Before testing the effect of the drug on the cells seeded on the BioChip 4096E by impedance monitoring, it was necessary to test it on a classic tissue-culture 12-well plate (Corning®), in order to assess the effect of different Etoposide concentrations on the cell culture by fluorescence microscopy. Eight wells of the well plate were used and the protocol respected is described below:

1. The culture wells was seeded each one with 50000 cells, in 1 mL of culture medium.
2. After 24 hours from seeding, Etoposide was added in the eight culture wells at concentration respectively 0  $\mu\text{M}$ , 5  $\mu\text{M}$ , 10  $\mu\text{M}$ , 20  $\mu\text{M}$ , 40  $\mu\text{M}$ , 60  $\mu\text{M}$ , 80  $\mu\text{M}$ , 100  $\mu\text{M}$ .
3. After 24 hours of incubation, the medium containing Etoposide was removed and replaced with fresh medium.
4. After 24 hours from drug removal, a fluorescence microscopy analysis was conducted to find eventual evidences of apoptosis in the cell cultures.

For preparing the samples for the microscopy analysis, a labelling was executed on cells through a *In Situ Cell Death Detection Kit* with TMR red (*Sigma-Aldrich*®). This kit allows the detection of apoptosis by labelling only that DNA strand breaks caused by apoptosis, discriminating apoptosis from necrosis. The DNA damage caused during apoptosis can produce double-stranded DNA fragments or single strand breaks ("nicks"). The detection kit contains a label solution (labelled nucleotides) and an enzyme solution

(for catalysing the labelling reaction). It exploits the DNA single strand breaks, by labelling them with TMR (tetramethylrhodamine) red-labeled nucleotides (TMR-dUTPs) which attach to the 3'-OH ends of the single strands. This reaction is catalysed by the terminal deoxynucleotidyl transferase (TdT) enzyme and for this reason it is called *TUNEL* reaction (TdT-mediated dUTP nick end labeling). The protocol for the TUNEL assay is now listed [48]:

1. Fixation: cells are fixed for 1 hour with the fixation solution (4% Paraformaldehyde in PBS).
2. Washing: cells are washed twice with PBS.
3. Permeabilisation: it is conducted for 2 minutes by incubating cells in a permeabilisation solution (0.1% Triton X-100 in 0.1% sodium citrate).
4. Washing: cells are washed twice with PBS.
5. TUNEL mixture preparation: it is obtained by mixing 50  $\mu L$  of enzyme solution with 450  $\mu L$  of label solution.
6. Labeling reaction: for each well-plate 50  $\mu L$  of the labelling solution are added and incubated for 1 hour in the dark.
7. Washing: the culture plates are washed 3 times with PBS.
8. Fluorescence microscopy analysis.

Once the labeling was executed, the fluorescence analysis was conducted (*Carl Zeiss Microscopy* GmbH, Germany) to assess apoptosis in the eight treated culture plates. Some qualitative results are reported in figure 5.4.

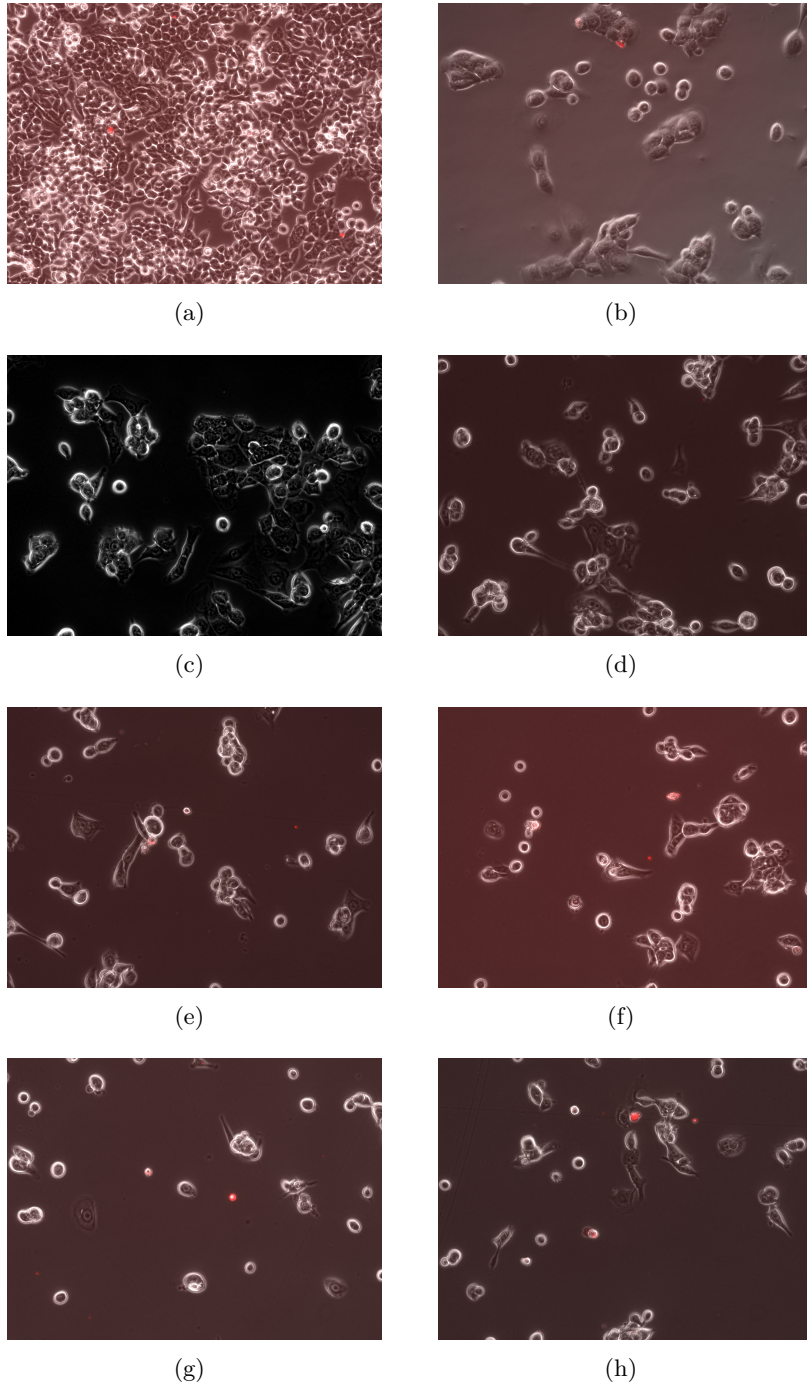


Figure 5.4: *Zeiss* Microscopy images (20 X) of the eight culture wells treated with Etoposide. a) ETO 0  $\mu M$ ; b) 5  $\mu M$ ; c) 10  $\mu M$ ; d) 20  $\mu M$ ; e) 40  $\mu M$ ; f) 60  $\mu M$ ; g) 80  $\mu M$ ; h) 100  $\mu M$ .

As expected, at  $0 \mu M$  cells reach the maximum confluence after 48 hours, with no signs of apoptosis. From  $5 \mu M$  some apoptosis signs are already evident and a confluence decrease is visible, index that a certain number of cells have become apoptotic and have been washed away during the washing steps with PBS in the labelling assay. The cells marked with red are cells which are becoming apoptotic and will detach soon.

However this validation method was useful only for a preliminar qualitative demonstration that ETO acts on HT-29 cells and that apoptosis occurs, since the confluence strongly decreases in all the cases. Instead, for having quantitative results another assay was conducted, the Guava Nexin® assay, which will be explained in the validation section.

After assessing that Etoposide is toxic for HT-29 cells, the impedance monitoring was conducted, testing four different ETO concentrations:  $0 \mu M$ ,  $10 \mu M$ ,  $20 \mu M$ ,  $40 \mu M$ . Etoposide was added to the cell culture after 20 hours from seeding, i.e. in the exponential phase of their growth. What is expected from the measurements is an impedance decrease during time after drug's administration due to apoptosis of cells and their subsequent detachment from the electrodes area [12].

Even in these experiments, the monitoring lasted 120 hours and figure 5.5 shows the results obtained: the first part of the curves (a) is referred to the preconditioning phase, followed by the slow growth phase (b); the third portion is referred to the exponential growth (c); after 20 hours ETO was added to the cell culture (d) and incubated for 24 hours. Once spent 24 hours, the drug was removed (e) and the remaining part of the curve (f) is referred to the monitoring after drug removal.

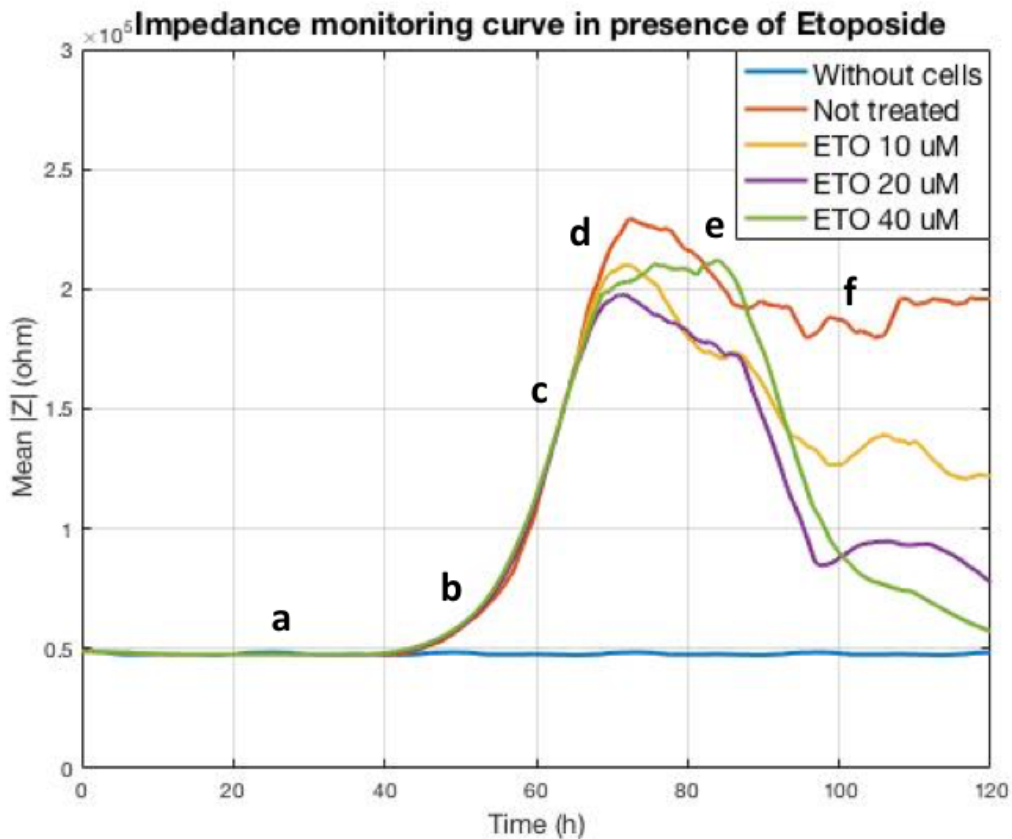


Figure 5.5: **Impedance curves obtained from the monitoring of the BioChip's cell culture treated with Etoposide.** Different concentrations were tested:  $0 \mu M$ ,  $10 \mu M$ ,  $20 \mu M$ ,  $40 \mu M$ , added to the case of culture medium without cells.

Because of ETO's action, cells start dying and detaching, determining an impedance diminution over time. A dose-dependent effect can be observed: the impedance diminution is more accentuated in the case "40  $\mu M$ " because a greater number of cells become apoptotic. However, as can be seen from the graph, differently from the cases "10  $\mu M$ " and "20  $\mu M$ ", impedance stay high during the phase "e": this can be explained to be due to the high number of cells that detach from the electrodes but remain in the culture medium until the drug is removed, preventing the current flow. When the drug is removed and replaced with fresh medium, the detached cells are aspirated and impedance starts a steep decrease.

### 5.2.1 Validation assay

For demonstrating that the BioChip's impedance measurements provide reliable results, a validation test was conducted, the Guava Nexin® Assay, for a quantitative analysis of apoptosis occurrence in presence of Etoposide. The principle exploited by this assay is one of the effects of apoptosis on cells, i.e. the externalization of phosphatidylserine (PS), a component of the cell membrane which in normal conditions is localized in the cytoplasmic domain of the membrane.

The Guava Nexin® Reagent is a mixture of two fluorescent markers [49]:

- Annexin V-PE is a phospholipid-binding protein which binds to PS when it is in the external domain of the cell membrane, i.e. when the cell is apoptotic.
- 7-AAD (7-amino-actinomycin D) is a marker of the membrane integrity, which binds to the DNA when the cell membrane is damaged; it is used for distinguishing late apoptotic cells from early apoptotic or non apoptotic cells.

Table 5.2 reports the different populations of cells which this assay can distinguish, through the Annexin V and 7-AAD binding.

Table 5.2: Populations of cells which can be distinguished by the Guava Nexin® Assay. [49]

Cells population	Annexin V	7-AAD
Non apoptotic cells	-	-
Early apoptotic cells	+	-
Late apoptotic and dead cells	+	+

For executing this assay another 12-well plate (Corning®) was employed and each well was seeded with 50000 cells. After 20 hours from seeding, ETO was added to eight wells for obtaining the percentage of apoptotic cells for each ETO concentration (0  $\mu M$ , 5  $\mu M$ , 10  $\mu M$ , 20  $\mu M$ , 40  $\mu M$ , 60  $\mu M$ , 80  $\mu M$ , 100  $\mu M$ ). After 24 hours of incubation the drug was removed, exactly as for BioChip's protocols, and the labelling procedure for the Guava Nexin® Assay was started.

The labelling protocol was conducted as follows [49]:

1. Cells in the wells were detached by trypsin and collected in eight 15 mL Falcon™ tubes, together with their culture medium;
2. The tubes were centrifuged at 1000 rpm for 5 minutes;

3. The medium was aspirated and the pellet was resuspended in  $50 \mu L$  of fresh medium in an eppendorf;
4. Cells of each tube were counted and eventually diluted because the protocol requires a number of cells from 20000 to 100000 per sample;
5. The final volume for each sample was carried to  $50 \mu L$  and  $50 \mu L$  of the labelling solution were added;
6. The samples were stained in the dark for 20 minutes at room temperature;
7. The samples were ready for the analysis.

Once stained, the samples were analyzed one by one by inserting them into the loader of the Muse® Cell Analyzer, a miniaturized system for fluorescence detection and microcapillary cytometry. After loading the sample, the user interface on the instrument allows to regulate the settings, establishing the population profile for the sample. Then the system is ready for the acquisition. At the end of the acquisition, the results are shown in form of dotplots and statistics. In the following figure (5.6), the instrument design and an example of the results are reported.

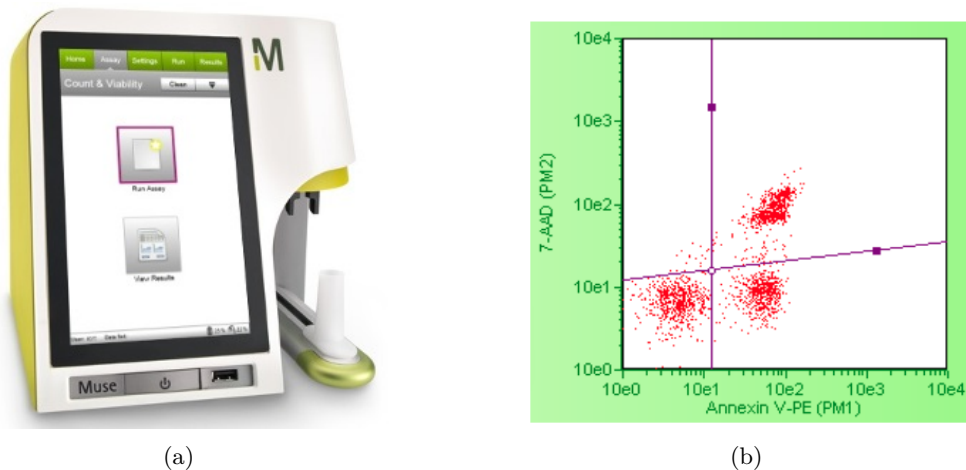


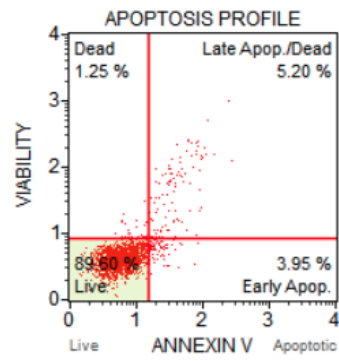
Figure 5.6: a) **Design of the Muse® Cell Analyzer** [50]; b) **Example of the results provided by the instrument's analysis** [49].

As shown in figure, a graph is displayed and divided into four quadrants. These quadrants are organized in this way:

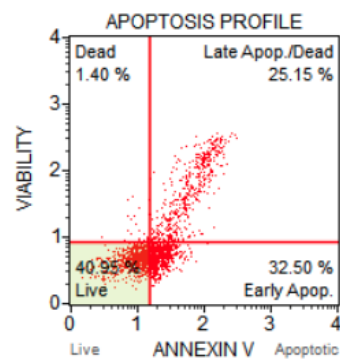
- Lower-left quadrant contains non apoptotic cells;
- Lower-right quadrant includes the early apoptotic cells;
- Upper-right quadrant contains the late apoptotic or dead cells;
- Upper-left quadrant includes cellular debris.

The statistics displayed together with the graph provide a percentage of each cells population.

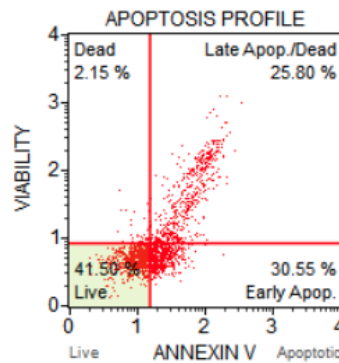
In figure 5.7 the results obtained for the concentrations of Etoposide tested on the cell cultures.



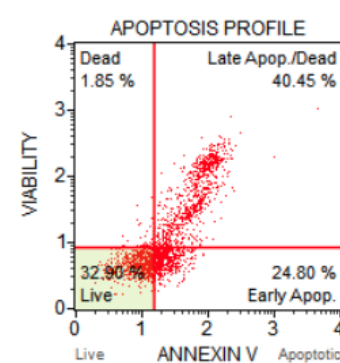
(a)



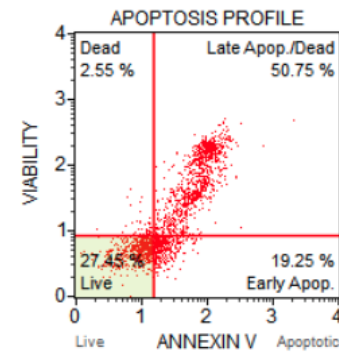
(b)



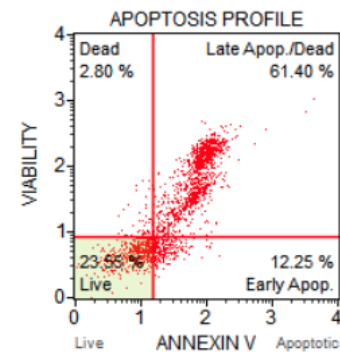
(c)



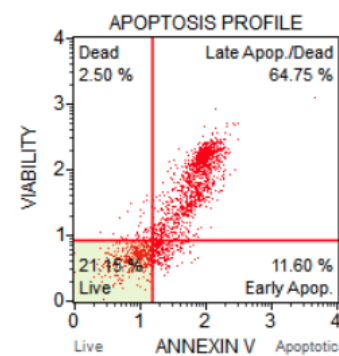
(d)



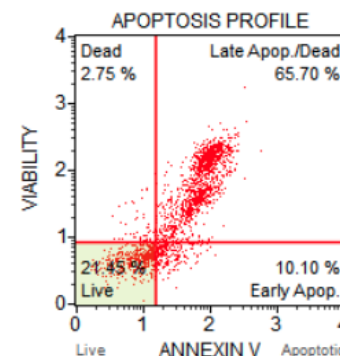
(e)



(f)



(g)



(h)

Figure 5.7: Results of the Muse™ Cell Analyzer analysis. a) ETO 0  $\mu M$ ; b) 5  $\mu M$ ; c) 10  $\mu M$ ; d) 20  $\mu M$ ; e) 40  $\mu M$ ; f) 60  $\mu M$ ; g) 80  $\mu M$ ; h) 100  $\mu M$ .

As visible from figure 5.7 and evidenced in figure 5.8, the apoptosis induction by Etoposide is already pronounced at low concentrations ( $5 \mu M$ ) and tends to slightly increase with the drug's concentration. In particular, a difference in apoptosis percentage can be seen comparing the concentrations  $0 \mu M$ ,  $10 \mu M$ ,  $20 \mu M$  and  $40 \mu M$ . This is in accordance with the impedance measurements obtained on the BioChip, demonstrating that the developed system gives reliable results.

As can be seen from the quadrants showed in figure 5.7, if the drug's dose is too high, the percentage of early apoptotic cells decreases, while the percentage of late apoptotic/necrotic cells increases: this is index of cell necrosis, due to a toxic dose of Etoposide.

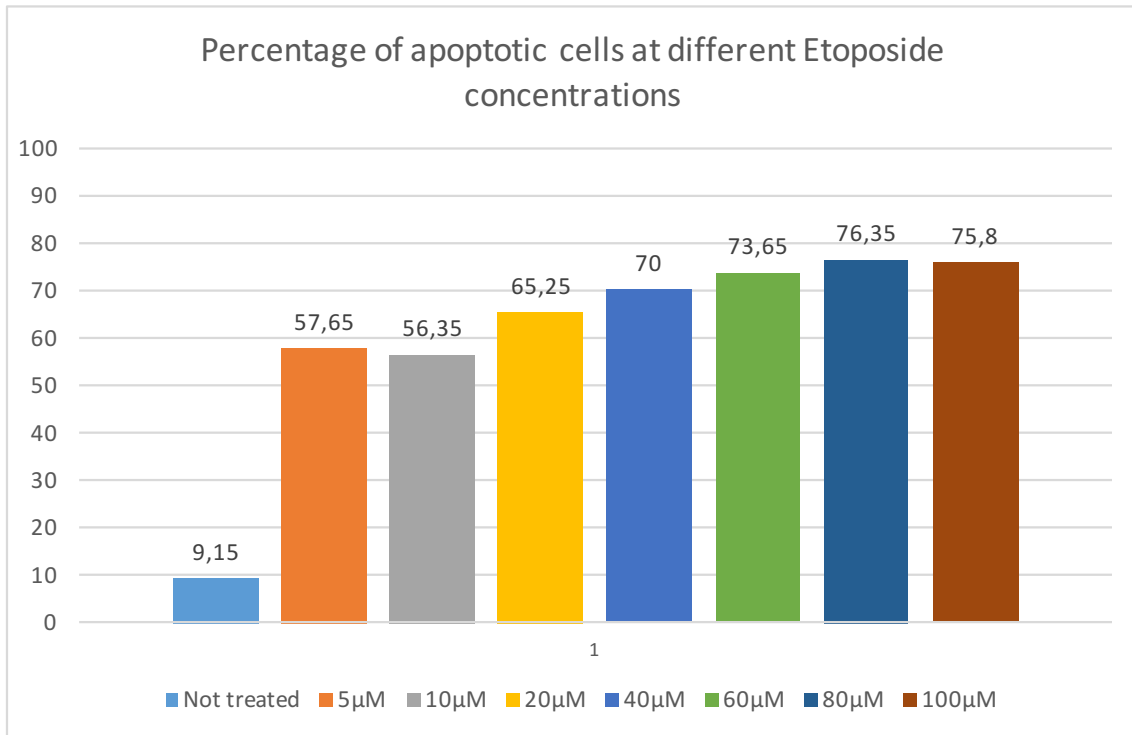


Figure 5.8: Bar graph showing the apoptotic cells percentages for each sample analysed.

## Chapter 6

# Conclusions and future perspectives

The objective of this thesis work was the implementation of a system for the measurement of impedance through the electric cell-substrate impedance sensing (ECIS) technique, with the aim of monitoring cell activities, such as adhesion, proliferation and apoptosis, due to the presence of a drug. In contrast with the traditional laboratory assays used for drug screening, this method is label-free, non-invasive and real-time, hence it can offer many advantages in drug screening studies, not only in terms of time-saving, but also in terms of economic savings.

The experimental set-up consisted of a personal computer with the integrated development environments necessary for the measurements, the HT-29 cell line, an impedance analyzer and the BioChip 4096 from *3Brain*. A graphical user interface was created in LabVIEW® to control the impedance analyzer and the Arduino® IDE was used to program an Arduino® Micro for the choice of the electrodes for conducting the measurement. Firstly, it was necessary to optimize the cell seeding protocol in the culture chamber of BioChip 4096, in terms of number of cells and quantity of collagen type I and laminin to improve adhesion. The best adhesion degree was provided by the experiment in which 50000 cells, 10  $\mu\text{g}/\text{mL}$  of collagen type I and 10  $\mu\text{g}/\text{mL}$  of laminin were used.

Once obtained the best result through fluorescence microscopy, the impedance measurement was executed, for evaluating if the impedance curve followed the trend of the cellular growth curve, with a *lag phase*, a *log phase* and a *stationary phase*. Good results were obtained: by studying the impedance curve it is possible to distinguish cellular adhesion, proliferation and the achievement of a plateau, due to confluence or nutrients exhaustion. The second part of the work was focused on drug screening experiments, using Etoposide, a drug which induces apoptosis by nuclear fragmentation. It was added to the cell culture in the exponential phase of the growth and at different concentrations. As expected, impedance started decreasing after drug addition, showing a dose-dependent effect; this effect was in strict accordance with the results obtained through microscopy analysis.

These results demonstrate that ECIS may be a good candidate to preliminar *in vitro* drug screening studies, in order to reduce the exploitation of animal models in the preclinical phase.

For these reasons, impedance could become in future an auxiliary technique in the early steps of the drug discovery process. A possible improvement for the platform developed in my master thesis work could be aimed to guarantee a better portability of the system, now

not allowed, mainly due to the heaviness of the impedance analyzer. Additionally, another possibility could be the integration of the electronic circuitry for measuring impedance directly within the chip's PCB. Moreover, other cell lines could be seeded or different molecules or drugs could be tested, to consolidate the reliability of this system.

# Bibliography

- [1] Dmitri V. Krysko, Tom Vanden Berghe, Katharina D’Herde, Peter Vandenabeele, *Apoptosis and necrosis: Detection, discrimination and phagocytosis*, *Methods* (44), 205-221, 2008.
- [2] Tohru Yonekawa, Andrew Thorburn, *Autophagy and Cell Death*, *Essays Biochem.* (55), 105-117, 2013.
- [3] Susan Elmore, *Apoptosis: A Review of Programmed Cell Death*, *Toxicologic Pathology* (35), 495-516, 2007.
- [4] Rebecca SY Wong, *Apoptosis in cancer: from pathogenesis to treatment*, *Journal of Experimental & Clinical Cancer Research* (30), 2011.
- [5] Claire M. Pfeffer, Amareshwar T. K. Singh, *Apoptosis: A Target for Anticancer Therapy*, *International Journal of Molecular Sciences* (19), 448-457, 2018.
- [6] How Chemotherapy Drugs Work. <https://www.cancer.org/treatment/treatments-and-side-effects/treatment-types/chemotherapy/how-chemotherapy-drugs-work.html>.
- [7] Gerard I. Evan, Karen H. Vousden, *Proliferation, cell cycle and apoptosis in cancer*, *Nature* (411), 342-348, 2001.
- [8] Seila Selimovic, Mehmet R. Dokmeci, Ali Khademhosseini, *Organs-on-a-chip for drug discovery*, *Current Opinion in Pharmacology* (13), 829-833, 2013.
- [9] Youchun Xu, Xinwu Xie, Yong Duan, Lei Wang, Zhen Cheng, Jing Cheng, *A review of impedance measurements of whole cells*, *Biosensors and Bioelectronics* (77), 824-836, 2016.
- [10] Cellular impedance explained. <https://www.aceabio.com/products/icelligence/>.
- [11] Szulcek R., Bogaard H.J., Van Nieuw Amerongen G.P., *Electric Cell-substrate Impedance Sensing for the Quantification of Endothelial Proliferation, Barrier Function, and Motility*, *J. Vis. Exp.* (85), 2014.
- [12] Jessica Ponti, Laura Ceriotti, Barbara Munaro, Massimo Farina, Alessio Munari, Maurice Whelan, Pascal Colpo, Enrico Sabbioni and François Rossi, *Comparison of Impedance-based Sensors for Cell Adhesion Monitoring and In Vitro Methods for Detecting Cytotoxicity Induced by Chemicals*, *ATLA* (34), 515–525, 2006.
- [13] Silke Arndt, Jochen Seebach, Katherina Psathaki, Hans-Joachim Galla, Joachim Wegener, *Bioelectrical impedance assay to monitor changes in cell shape during apoptosis*, *Biosensors and Bioelectronics* (19), 583-594, 2004.

- [14] ECIS theory. <http://www.biophysics.com/ecis-theory.php>.
- [15] Enric Sarró, Martí Lecina, Andreu Fontova, Francesc Godia, Ramon Bragós and Jordi J Cairó, *Real-time and on-line monitoring of morphological cell parameters using electrical impedance spectroscopy measurements*, Society of Chemical Industry, J. Chem. Technol. Biotechnol (91), 1755-1762, 2016.
- [16] The biopharmaceutical research and development process. [http://phrma-docs.phrma.org/sites/default/files/pdf/rd\\_brochure\\_022307.pdf](http://phrma-docs.phrma.org/sites/default/files/pdf/rd_brochure_022307.pdf).
- [17] The drug development process (U.S. Food and Drug administration website). <https://www.fda.gov/ForPatients/Approvals/Drugs/default.htm>.
- [18] Anna Astashkina, Brenda Mann, David W. Grainger, *A critical evaluation of in vitro cell culture models for high-throughput drug screening and toxicity*, Pharmacology & Therapeutics (134), 82-106, 2012.
- [19] S. Kustermann, F. Boess, A. Buness, M. Schmitz, M. Watzele, T. Weiser, T. Singer, L. Suter, A. Roth, *A label-free, impedance-based real time assay to identify drug-induced toxicities and differentiate cytostatic from cytotoxic effects*, Toxicology in Vitro (27), 1589-1595, 2013.
- [20] L. Ceriotti, J. Ponti, F. Broggi, A. Kob, S. Drechsler, E. Thedinga, P. Colpo, E. Sabbioni, R. Ehret, F. Rossi, *Real-time assessment of cytotoxicity by impedance measurement on a 96-well plate*, Sensors and Actuators B (123), 769-778, 2007.
- [21] Fareid Asphahani, Miqin Zhang, *Cellular Impedance Biosensors for Drug Screening and Toxin Detection*, Analyst. (132), 835-841, 2007.
- [22] Lei Wanga, Hongying Yina, Wanli Xinga, Zhongyao Yue, Min Guoe, Jing Cheng, *Real-time, label-free monitoring of the cell cycle with a cellular impedance sensing chip*, Biosensors and Bioelectronics (25), 990-995, 2010.
- [23] David Schneider, Marco Tarantola, Andreas Janshoff, *Dynamics of TGF- $\beta$  induced epithelial-to-mesenchymal transition monitored by Electric Cell-Substrate Impedance Sensing*, Biochimica et Biophysica Acta (1813), 2099-2107, 2011.
- [24] A. Ferrario, M. Scaramuzza, E. Pasqualotto, A. De Toni, A. Paccagnella, M. Maschietto, S. Vassanelli, *Electrochemical impedance spectroscopy study of the cells adhesion over microelectrodes array*, IEEE, 2011.
- [25] Ju Hun Yeon, Je-Kyun Park, *Cytotoxicity test based on electrochemical impedance measurement of HepG2 cultured in microfabricated cell chip*, Analytical Biochemistry (341), 308-315, 2005.
- [26] Amin H, Maccione A, Marinaro F, Zordan S, Nieuw T and Berdondini L, *Electrical Responses and Spontaneous Activity of Human iPS-Derived Neuronal Networks Characterized for 3-month Culture with 4096-Electrode Arrays*. Frontiers in Neuroscience (10), article n.121, 2016.
- [27] HD MEA Probes. <http://3brain.com/mea.html>.

- [28] A. Maccione, A. Simi, T. Nieuw, M. Gandolfo, K. Imfeld, E. Ferrea, E. Sernagor and L. Berdondini, *Sensing and actuating electrophysiological activity on brain tissue and neuronal cultures with a high-density CMOS-MEA*, Conference paper, Solid-State Sensors, Actuators and Microsystems (TRANSDUCERS & EUROSENSORS XXVII), 2013.
- [29] Maccione A, Berdondini L, *Standard protocol for dissociated cultures on BioChips*, version 1.2.1, 2013. <http://3brain.com/downloads.html> .
- [30] HT-29 ATCC® product datasheet. [https://www.lgcstandards-atcc.org/Products/All/HTB-38.aspx?geo\\_country=it#documentation](https://www.lgcstandards-atcc.org/Products/All/HTB-38.aspx?geo_country=it#documentation).
- [31] Daniel Martinez-Maqueda, Beatriz Miralles, Isidra Recio, *HT29 Cell Line*, The impact of Food Bio-Actives on Gut Health, chapter 11, 113-123, 2015.
- [32] Cell culture basics handbook (Invitrogen). <http://www.thermofisher.com/it/en/home/references/gibco-cell-culture-basics.html?cid=f1-cellculturebasics>.
- [33] *Thawing, Propagating and Cryopreserving Protocol*, version 1.6, 2012. [https://physics.cancer.gov/docs/bioresource/colorectal/NCI-PBCF-HTB38\\_HT-29\\_SOP-508.pdf](https://physics.cancer.gov/docs/bioresource/colorectal/NCI-PBCF-HTB38_HT-29_SOP-508.pdf) .
- [34] Ilona Schonn, Jana Hennesen, Dorothee C. Dartsch, *Cellular responses to etoposide: cell death despite cell cycle arrest and repair of DNA damage*, Apoptosis (15), 162-172, 2010.
- [35] Alessandra Montecucco, Giuseppe Biamonti, *Cellular response to etoposide treatment*, Cancer Letters (252), 9-18, 2007.
- [36] Kenneth D. Bromberg, Alex B. Burgin, and Neil Osheroff, *A Two Drug Model for Etoposide Action Against Human Topoisomerase II $\alpha$* , Journal of Biological Chemistry (278), 7406-7412, 2002.
- [37] E. L. Baldwin, N. Osheroff, *Etoposide, Topoisomerase II and Cancer*, Current Medicinal Chemistry - Anti-Cancer Agents (5), 363-372, 2005.
- [38] Agilent Technologies, *Agilent Impedance Measurement Handbook - A guide to measurement technology and techniques*, 4th Edition, printed in USA, 2009.
- [39] 4294A Precision Impedance Analyzer, 40 Hz to 110 MHz. <https://www.keysight.com/en/pd-1000000858%3Aepsg%3Apro-pn-4294A/precision-impedance-analyzer-40-hz-to-110-mhz?cc=US&lc=eng>.
- [40] 16089B Medium Kelvin Clip Lead. <https://www.keysight.com/en/pd-1000000489%3Aepsg%3Apro-pn-16089B/medium-kelvin-clip-lead?nid=-34051.536879617&cc=IT&lc=ita>.
- [41] Arduino Micro documentation. <https://store.arduino.cc/usa/arduino-micro>.
- [42] CD4067B CMOS analog multiplexers datasheet. <http://www.ti.com/lit/ds/symlink/cd4067b.pdf>.
- [43] Arduino® Micro pinout. [https://www.arduino.cc/en/uploads/Main/ArduinoMicro\\_Pinout3.png](https://www.arduino.cc/en/uploads/Main/ArduinoMicro_Pinout3.png).

- [44] Luciana Stanica, Mihnea Rosu-Hamzescu, Mihaela Gheorghiu, Miruna Stan, Loredana Antonescu, Cristina Polonschii, Eugen Gheorghiu, *Electric Cell-Substrate Impedance Sensing of Cellular Effects under Hypoxic Conditions and Carbonic Anhydrase Inhibition*, Journal of Sensors (17), 2017.
- [45] Daniel Opp, Brian Wafula, Jennifer Lim, Eric Huang, Jun-Chih Lo, and Chun-Min Lo, *Use of electric cell-substrate impedance sensing to assess in vitro cytotoxicity*, Biosensors and Bioelectronic (24), 2625-2629, 2009.
- [46] Kin Fong Lei, Min-Hsien Wu, Che-Wei Hsu, Yi-Dao Chen, *Real-time and non-invasive impedimetric monitoring of cell proliferation and chemosensitivity in a perfusion 3D cell culture microfluidic chip*, Biosensors and Bioelectronics (51), 16-21, 2014.
- [47] Vybrant® CFDA SE Cell Tracer Kit, January 2006. <https://www.thermofisher.com/order/catalog/product/V12883>.
- [48] *In Situ Cell Death Detection Kit, TMR red*, version 12, March 2016. <https://www.sigmaaldrich.com/content/dam/sigma-aldrich/docs/Roche/Bulletin/1/12156792910bul.pdf>
- [49] Guava Nexin Reagent for Flow Cytometry. [http://www.merckmillipore.com/IT/it/product/Guava-Nexin-Reagent-for-Flow-Cytometry-100-tests,MM\\_NF-4500-0450?ReferrerURL=https%3A%2F%2Fwww.google.it%2F&bd=1#anchor\\_DS](http://www.merckmillipore.com/IT/it/product/Guava-Nexin-Reagent-for-Flow-Cytometry-100-tests,MM_NF-4500-0450?ReferrerURL=https%3A%2F%2Fwww.google.it%2F&bd=1#anchor_DS).
- [50] Muse™ Cell Analyzer. [http://www.merckmillipore.com/IT/it/life-science-research/cell-analysis-flow-cytometry/muse-cell-analyzer/hb2b.qB.1I0AAAE\\_vzlkifKv.nav](http://www.merckmillipore.com/IT/it/life-science-research/cell-analysis-flow-cytometry/muse-cell-analyzer/hb2b.qB.1I0AAAE_vzlkifKv.nav).